

QD  
461  
I'67  
1992  
C.2

# INTERMOLECULAR AND SURFACE FORCES

SECOND EDITION

JACOB N. ISRAELACHVILI

Department of Chemical & Nuclear Engineering  
and Materials Department  
University of California, Santa Barbara  
California, USA

MIL



ACADEMIC PRESS

Harcourt Brace Jovanovich, Publishers  
London San Diego New York Boston  
Sydney Tokyo Toronto

ACADEMIC PRESS LIMITED  
24–28 Oval Road  
London NW1 7DX

United States Edition published by  
ACADEMIC PRESS INC.  
San Diego, CA 92101

Copyright © 1992 by  
ACADEMIC PRESS LIMITED

First Edition published in 1985  
Second Edition 1991

All Rights Reserved.  
No part of this book may be reproduced in any form,  
by photostat, microfilm or any other means,  
without written permission from the publishers

A catalogue record for this book is available  
from the British Library

ISBN 0-12-375181-0

Typeset by P&R Typesetters Ltd, Salisbury, Wiltshire  
Printed by St Edmundsbury Press Ltd, Bury St Edmunds, Suffolk

## Contents

### PART ONE

## The Forces Between Atoms and Molecules: Principles and Concepts

<b>Chapter 1</b>	<b>Historical Perspective</b>	<b>3</b>
1.1	The four forces of nature	3
1.2	Greek and medieval notions of intermolecular forces	3
1.3	Early scientific period: contrasts with gravitational forces	5
1.4	First successful phenomenological theories	8
1.5	Modern view of the origin of intermolecular forces	11
1.6	Recent trends	11
	<i>Problems and discussion topics</i>	
<b>Chapter 2</b>	<b>Some Thermodynamic Aspects of Intermolecular Forces</b>	<b>16</b>
2.1	Interaction energies of molecules in free space and in a medium	16
2.2	The Boltzmann distribution	20
2.3	The distribution of molecules and particles in systems at equilibrium	21
2.4	The van der Waals equation of state	23
2.5	The criterion of the thermal energy $kT$ for gauging the strength of an interaction	24
2.6	Classification of forces	27
	<i>Problems and discussion topics</i>	
<b>Chapter 3</b>	<b>Strong Intermolecular Forces: Covalent and Coulomb Interactions</b>	<b>31</b>
3.1	Covalent or chemical bonding forces	31
3.2	Physical and chemical bonds	32

## CONTENTS

3.3 Coulomb forces or charge–charge interactions	32
3.4 Ionic crystals	35
3.5 Reference states	36
3.6 Range of Coulomb forces	36
3.7 The Born energy of an ion	37
3.8 Solubility of ions in different solvents	38
3.9 Specific ion–solvent effects	42
3.10 Continuum approach	43
3.11 Molecular approach: computer simulations <i>Problems and discussion topics</i>	44
<b>Chapter 4 Interactions Involving Polar Molecules</b>	<b>48</b>
4.1 What are polar molecules?	48
4.2 Dipole self-energy	50
4.3 Ion–dipole interactions	50
4.4 Ions in polar solvents	54
4.5 Strong ion–dipole interactions: hydrated ions	55
4.6 Solvation forces, structural forces, hydration forces	56
4.7 Dipole–dipole interactions	57
4.8 Rotating dipoles and angle-averaged potentials	60
4.9 Entropic effects <i>Problems and discussion topics</i>	63
<b>Chapter 5 Interactions Involving the Polarization of Molecules</b>	<b>67</b>
5.1 The polarizability of atoms and molecules	67
5.2 The polarizability of polar molecules	70
5.3 Interactions between ions and uncharged molecules	71
5.4 Ion–solvent molecule interactions and the Born energy	73
5.5 Dipole-induced dipole interactions	74
5.6 Unification of polarization interactions	75
5.7 Solvent effects and ‘excess polarizabilities’ <i>Problems and discussion topics</i>	76
<b>Chapter 6 van der Waals Forces</b>	<b>83</b>
6.1 Origin of the van der Waals dispersion force between neutral molecules: the London equation	83
6.2 Strength of dispersion forces: van der Waals solids and liquids	85
6.3 van der Waals equation of state	90
6.4 Gas–liquid and liquid–solid phase transitions	91
6.5 van der Waals forces between polar molecules	93
6.6 General theory of van der Waals forces between molecules	96

## CONTENTS

6.7 van der Waals forces in a medium	99
6.8 Dispersion self-energy of a molecule in a medium	103
6.9 Further aspects of van der Waals forces: anisotropy, non-additivity and retardation effects <i>Problems and discussion topics</i>	105
<b>Chapter 7 Repulsive Forces, Total Intermolecular Pair Potentials and Liquid Structure</b>	<b>109</b>
7.1 Sizes of atoms, molecules and ions	109
7.2 Repulsive potentials	112
7.3 Total intermolecular pair potentials	113
7.4 Role of repulsive forces in non-covalently bonded solids	115
7.5 Role of repulsive forces in liquids: liquid structure	117
7.6 Effect of liquid structure on molecular forces <i>Problems and discussion topics</i>	119
<b>Chapter 8 Special Interactions: Hydrogen-Bonding, Hydrophobic and Hydrophilic Interactions</b>	<b>122</b>
8.1 The unique properties of water	122
8.2 The hydrogen bond	123
8.3 Models of water and associated liquids	125
8.4 Relative strengths of different types of interactions	127
8.5 The hydrophobic effect	128
8.6 The hydrophobic interaction	131
8.7 Hydrophilicity <i>Problems and discussion topics</i>	133
<b>PART TWO</b>	
<b>The Forces Between Particles and Surfaces</b>	
<b>Chapter 9 Some Unifying Concepts in Intermolecular and Interparticle Forces</b>	<b>139</b>
9.1 Factors favouring the association of like molecules or particles in a medium	139
9.2 Two like surfaces coming together in a medium: surface and interfacial energy	144
9.3 Factors favouring the association of unlike molecules, particles or surfaces in a third medium	145
9.4 Particle–surface interactions	147

9.5	Adsorbed surface films: wetting and non-wetting <i>Problems and discussion topics</i>	149
<b>Chapter 10</b>	<b>Contrasts Between Intermolecular, Interparticle and Intersurface Forces</b>	<b>152</b>
10.1	Short-range and long-range effects of a force	152
10.2	Interaction potentials between macroscopic bodies	155
10.3	Effective interaction area of two spheres: the Langbein approximation	159
10.4	Interactions of large bodies compared to those between molecules	159
10.5	Interaction energies and interaction forces: the Derjaguin approximation	161
10.6	Experimental measurements of intermolecular and surface forces	165
10.7	Direct measurements of surface and intermolecular forces <i>Problems and discussion topics</i>	168
<b>Chapter 11</b>	<b>van der Waals Forces Between Surfaces</b>	<b>176</b>
11.1	The force laws for bodies of different geometries: the Hamaker constant	176
11.2	Strength of van der Waals forces between bodies in vacuum or air	178
11.3	The Lifshitz theory of van der Waals forces	179
11.4	Hamaker constants calculated on the basis of the Lifshitz theory	183
11.5	Applications of the Lifshitz theory to interactions in a medium	188
11.6	Repulsive van der Waals forces: disjoining pressure and wetting films	192
11.7	Retardation effects	196
11.8	Screened van der Waals forces in electrolyte solutions	199
11.9	Combining relations	200
11.10	Surface and adhesion energies	201
11.11	Surface energies of metals	204
11.12	Forces between surfaces with adsorbed layers	206
11.13	Experiments on van der Waals forces <i>Problems and discussion topics</i>	207
<b>Chapter 12</b>	<b>Electrostatic Forces Between Surfaces in Liquids</b>	<b>213</b>
12.1	The charging of surfaces in liquids: the electric ‘double layer’	213

12.2	Charged surfaces in water (no added electrolyte)	215
12.3	The Poisson–Boltzmann (PB) equation	215
12.4	Surface charge, electric field and counterion concentration at a surface	217
12.5	Counterion concentration profile away from a surface	219
12.6	Origin of the ionic distribution, electric field, surface potential and pressure	221
12.7	The pressure between two charged surfaces in water: the contact value theorem	223
12.8	Limitations of the Poisson–Boltzmann equation	227
12.9	Thick wetting films	229
12.10	Limit of small separations: charge regulation	230
12.11	Charged surfaces in electrolyte solutions	231
12.12	The Grahame equation	233
12.13	Surface charge and potential in the presence of monovalent ions	234
12.14	Effect of divalent ions	237
12.15	The Debye length	238
12.16	Variation of potential and ionic concentrations away from a charged surface	239
12.17	The electrostatic double-layer interaction between charged surfaces in electrolyte	241
12.18	van der Waals and double-layer forces acting together: the DLVO theory	246
12.19	Experimental measurements of double-layer and DLVO forces	250
12.20	Effects of discrete surface charges and dipoles <i>Problems and discussion topics</i>	254
<b>Chapter 13</b>	<b>Solvation, Structural and Hydration Forces</b>	<b>260</b>
13.1	Non-DLVO forces	260
13.2	Molecular ordering at surfaces and interfaces and in thin films	261
13.3	Origin of main type of solvation force: the oscillatory force	265
13.4	Measurements and properties of solvation forces: oscillatory forces in non-aqueous liquids	269
13.5	Solvation forces in aqueous systems: repulsive ‘hydration’ forces	275
13.6	Solvation forces in aqueous systems: attractive ‘hydrophobic’ forces <i>Problems and discussion topics</i>	282
<b>Chapter 14</b>	<b>Steric and Fluctuation Forces</b>	<b>288</b>
14.1	Diffuse interfaces	288
14.2	Polymers at surfaces	289

14.3	Repulsive 'steric' or 'overlap' forces between polymer-covered surfaces	293
14.4	Forces in pure polymer liquids (polymer melts)	298
14.5	Attractive 'intersegment,' 'bridging' and 'depletion' forces	299
14.6	Non-equilibrium aspects of polymer interactions	303
14.7	Thermal fluctuation forces between fluid-like surfaces	304
14.8	Protrusion forces	304
14.9	Undulation and peristaltic forces	307
	<i>Problems and discussion topics</i>	
<b>Chapter 15</b>	<b>Adhesion</b>	<b>312</b>
15.1	Surface and interfacial energies	312
15.2	Surface energies of small clusters and highly curved surfaces	317
15.3	Contact angles and wetting films	319
15.4	Hysteresis in contact angle and adhesion measurements	322
15.5	Adhesion force between solid particles: the JKR and Hertz theories	326
15.6	Effect of capillary condensation on adhesion	330
	<i>Problems and discussion topics</i>	

**PART THREE****Fluid-Like Structures and Self-Assembling Systems:  
Micelles, Bilayers and Biological Membranes**

<b>Chapter 16</b>	<b>Thermodynamic Principles of Self-Assembly</b>	<b>341</b>
16.1	Introduction	341
16.2	Fundamental thermodynamic equations of self-assembly	345
16.3	Conditions necessary for the formation of aggregates	348
16.4	Variation of $\mu_N^0$ with N for simple structures of different geometries: rods, discs and spheres	349
16.5	The critical micelle concentration (CMC)	351
16.6	Infinite aggregates (phase separation) versus finite-sized aggregates (micellization)	352
16.7	Size distributions of self-assembled structures	354
16.8	More complex amphiphilic structures	360
16.9	Effects of interactions between aggregates: mesophases and multilayers	362
16.10	Conclusion	364
	<i>Problems and discussion topics</i>	

<b>Chapter 17</b>	<b>Aggregation of Amphiphilic Molecules into Micelles, Bilayers, Vesicles and Biological Membranes</b>	<b>366</b>
17.1	Introduction: equilibrium considerations of amphiphilic structures	366
17.2	Optimal headgroup area	367
17.3	Geometric packing considerations	370
17.4	Spherical micelles	371
17.5	Non-spherical and cylindrical micelles	374
17.6	Bilayers	375
17.7	Vesicles	378
17.8	Factors affecting changes from one structure to another	380
17.9	Curvature elasticity of bilayers and membranes	382
17.10	Biological membranes	385
17.11	Membrane lipids	387
17.12	Membrane proteins and membrane structure	389
	<i>Problems and discussion topics</i>	
<b>Chapter 18</b>	<b>The Interactions between Lipid Bilayers and Biological Membranes</b>	<b>395</b>
18.1	Introduction	395
18.2	Attractive van der Waals forces	395
18.3	Electrostatic (double-layer) forces	396
18.4	Hydration forces	399
18.5	Limitations of the hydration model	402
18.6	Steric forces	405
18.7	Hydrophobic forces	408
18.8	Specific interactions	410
18.9	Interdependence of intermembrane and intramembrane forces	412
18.10	Adhesion	414
18.11	Fusion	416
	<i>Problems and discussion topics</i>	
<b>References</b>		<b>422</b>
<b>Index</b>		<b>437</b>

In a book such as this, of modest size yet covering such a wide spectrum, it has not been possible to treat each topic exhaustively or rigorously, and specialists may find their particular subject discussed somewhat superficially.

The text is divided into three parts, the first dealing with the interactions between atoms and molecules, the second with the interactions between 'hard' particles and surfaces, and the third with 'soft' molecular aggregates in solution such as micelles (aggregates of surfactant molecules) and biological membranes (aggregates of lipids and proteins). While the fundamental forces are, of course, the same in each of these categories, they manifest themselves in sufficiently different ways that, I believe, they are best treated in three parts.

The primary aim of the book is to provide a thorough grounding in the theories and concepts of intermolecular forces so that the reader will be able to appreciate which forces are important in whatever system he or she is dealing with and to apply these theories correctly to specific problems (research or otherwise). The book is intended for final-year undergraduate students, graduate students, and non-specialist research workers.

I am deeply grateful to the following people who have read the text and made valuable comments for improving its presentation: Derek Chan, David Gruen, Bertil Halle, Roger Horn, Stjepan Marcelja, John Mitchell, Håkan Wennerström and Lee White. My thanks also extend to Diana Wallace for typing the manuscript and to Tim Sawkins for his careful drawing of most of the figures. But above all, I am indebted to my wife, Karin, without whose constant support this book would not have been written.

## UNITS AND SYMBOLS

Much of the published literature and equations on intermolecular and surface forces are based on the CGS system of units. In this book the *Système International* (SI) is used. In this system the basic units are the **kilogramme** (kg) for mass, the **metre** (m) for length, the **second** (s) for time, the **kelvin** (K) for temperature, the **ampère** (A) for electrical quantities, and the **mole** (mol) for quantity of mass. Some old units such as gramme ( $1 \text{ gm} = 10^{-3} \text{ kg}$ ), centimetre ( $1 \text{ cm} = 10^{-2} \text{ m}$ ), ångstrom ( $1 \text{ Å} = 10^{-10} \text{ m}$ ) and degree centigrade ( $^{\circ}\text{C}$ ) are still commonly used although they are not part of the SI system. The SI system has many advantages over the CGS, not least when it comes to forces. For example, force is expressed in newtons (N) without reference to the acceleration due to the earth's gravitation, which is implicit in some formulae based on the CGS system.

### DERIVED SI UNITS

Quantity	SI unit	Symbol	Definition of unit
Energy	Joule	J	$\text{kg m}^2 \text{s}^{-2}$
Force	Newton	N	$\text{kg m s}^{-2} = \text{J m}^{-1}$
Power	Watt	W	$\text{kg m s}^{-2} = \text{J s}^{-1}$
Pressure	Pascal	Pa	$\text{N m}^{-2}$
Electric charge	Coulomb	C	A s
Electric potential	Volt	V	$\text{J A}^{-1} \text{s}^{-1} = \text{J C}^{-1}$
Electric field	Volt/metre		$\text{V m}^{-1}$
Frequency	Hertz	Hz	$\text{s}^{-1}$

Fraction	$10^9$	$10^6$	$10^3$	$10^{-1}$	$10^{-2}$	$10^{-3}$	$10^{-6}$	$10^{-9}$	$10^{-12}$
Prefix symbol	G	M	k	d	c	m	$\mu$	n	p

## FUNDAMENTAL CONSTANTS

Constant	Symbol	SI	CGS
Avogadro's constant	$N_0$	$6.022 \times 10^{23} \text{ mol}^{-1}$	$6.022 \times 10^{23} \text{ mol}^{-1}$
Boltzmann's constant	$k$	$1.381 \times 10^{-23} \text{ J K}^{-1}$	$1.381 \times 10^{-16} \text{ erg deg}^{-1}$
Molar gas constant	$R = N_0 k$	$8.314 \text{ J K}^{-1} \text{ mol}^{-1}$	$8.314 \times 10^7 \text{ erg mol}^{-1} \text{ deg}^{-1}$
Electronic charge	$-e$	$1.602 \times 10^{-19} \text{ C}$	$4.803 \times 10^{-10} \text{ esu}$
Faraday constant	$F = N_0 e$	$9.649 \times 10^4 \text{ C mol}^{-1}$	$9.649 \times 10^4 \text{ C mol}^{-1}$
Planck's constant	$h (h = 2\pi\hbar)$	$6.626 \times 10^{-34} \text{ J s}$	$6.626 \times 10^{-27} \text{ erg s}$
Permittivity of free space	$\epsilon_0$	$8.854 \times 10^{-12} \text{ C}^2 \text{ J}^{-1} \text{ m}^{-1}$	$1$
Mass of $\frac{1}{12}$ of $^{12}\text{C}$ atom*	$u$	$1.661 \times 10^{-27} \text{ kg}$	$1.661 \times 10^{-24} \text{ g}$
Mass of hydrogen atom	$m_H$	$1.673 \times 10^{-27} \text{ kg}$	$1.673 \times 10^{-24} \text{ g}$
Mass of electron	$m_e$	$9.109 \times 10^{-31} \text{ kg}$	$9.109 \times 10^{-28} \text{ g}$
Gravitational constant	$G$	$6.670 \times 10^{-11} \text{ N m}^2 \text{ kg}^{-2}$	$6.670 \times 10^{-8} \text{ g}^{-1} \text{ cm}^3 \text{ s}^{-2}$
Speed of light in vacuum	$c$	$2.998 \times 10^8 \text{ m s}^{-1}$	$2.998 \times 10^{10} \text{ cm s}^{-1}$

\* Atomic mass unit (also denoted by a.m.u. and a.u.).

## CONVERSION FROM CGS TO SI

1 Å (ångstrom) = $10^{-10} \text{ m} = 10^{-8} \text{ cm} = 10^{-4} \mu\text{m} = 10^{-1} \text{ nm}$
1 litre = $10^{-3} \text{ m}^3 = 1 \text{ dm}^3$
1 erg = $10^{-7} \text{ J}$
1 cal = $4.184 \text{ J}$
1 kcal mol $^{-1}$ = $4.184 \text{ kJ mol}^{-1}$
1 kT = $4.114 \times 10^{-14} \text{ erg} = 4.114 \times 10^{-21} \text{ J}$ at 298 K ( $\sim 25^\circ\text{C}$ )
$= 4.045 \times 10^{-14} \text{ erg} = 4.045 \times 10^{-21} \text{ J}$ at 293 K ( $\sim 20^\circ\text{C}$ )
1 kT per molecule = $0.592 \text{ kcal mol}^{-1} = 2.478 \text{ kJ mol}^{-1}$ at 298 K
1 eV = $1.602 \times 10^{-12} \text{ erg} = 1.602 \times 10^{-19} \text{ J}$
1 eV per molecule = $23.06 \text{ kcal mol}^{-1} = 96.48 \text{ kJ mol}^{-1}$
1 cm $^{-1}$ (wavenumber unit of energy) = $1.986 \times 10^{-23} \text{ J}$
1 dyne = $10^{-5} \text{ N}$
1 dyne cm $^{-1}$ = 1 erg cm $^{-2}$ = 1 mN m $^{-1}$ = 1 mJ m $^{-2}$ (unit of surface tension)
1 dyne cm $^{-2}$ = $10^{-1} \text{ Pa (N m}^{-2}\text{)}$
1 atm = $1.013 \times 10^6 \text{ dyne cm}^{-2} = 1.013 \text{ bar} = 1.013 \times 10^5 \text{ Pa (N m}^{-2}\text{)}$
1 torr = 1 mm Hg = $1.316 \times 10^{-3} \text{ atm} = 133.3 \text{ Pa (N m}^{-2}\text{)}$
0°C = 273.15 K (triple point of water)
1 esu = $3.336 \times 10^{-10} \text{ C}$
1 poise (P) = $10 \text{ gm cm}^{-1} \text{ s}^{-1} = 10^{-1} \text{ kg m}^{-1} \text{ s}^{-1} = 10^{-1} \text{ N s m}^{-1}$ (unit of viscosity)

1 stokes (St) =  $10^{-4} \text{ m}^2 \text{ s}^{-1}$  (unit of kinematic viscosity: viscosity/density)  
 Debye (D) =  $10^{-18} \text{ esu} = 3.336 \times 10^{-30} \text{ C m}$  (unit of electric dipole moment)

## CONVERSION FROM SI TO CGS

1 nm = $10^{-9} \text{ m} = 10 \text{ \AA} = 10^{-7} \text{ cm}$
1 J = $10^7 \text{ erg} = 0.239 \text{ cal} = 6.242 \times 10^{18} \text{ eV}$
$= 5.034 \times 10^{22} \text{ cm}^{-1} = 7.243 \times 10^{22} \text{ K}$
1 kJ mol $^{-1}$ = $0.239 \text{ kcal mol}^{-1}$
1 N = $10^5 \text{ dyne}$
1 Pa = $1 \text{ N m}^{-2} = 9.872 \times 10^{-6} \text{ atm} = 7.50 \times 10^{-3} \text{ torr} = 10 \text{ dyne cm}^{-2}$
1 bar = $10^5 \text{ N m}^{-2} = 10^{-5} \text{ Pa} = 0.9868 \text{ atm} = 750.06 \text{ mm Hg}$

## USEFUL QUANTITIES AND RELATIONS

Energy equivalent, $mc^2$ , of one atomic mass unit (u) = $1.492 \times 10^{-10} \text{ J}$
Mean volume occupied per molecule = $(\text{MW})/(N_0 \times \text{density})$
Mass of any atom or molecule = $(\text{MW}) \times (1.661 \times 10^{-27}) \text{ kg}$
Standard volume of ideal gas = $22.414 \text{ m}^3 \text{ mol}^{-1} (1 \text{ mol}^{-1})$
kT/e = RT/F = $-25.69 \text{ mV}$ at 298 K
1 C m $^{-2}$ = 1 unit charge per $0.16 \text{ nm}^2 (16 \text{\AA}^2)$
$\kappa^{-1}$ (Debye length) = $0.304/\sqrt{\text{M}}$ nm for 1:1 electrolyte at 298 K, where $1 \text{ M} = 1 \text{ mol dm}^{-3} \equiv 6.022 \times 10^{26} \text{ molecules per m}^3$
Mass of the earth = $5.976 \times 10^{24} \text{ kg}$
Density of earth (mean) = $5.518 \times 10^3 \text{ kg m}^{-3}$
Values of gravitational acceleration, g: Equator ( $9.780 \text{ m s}^{-2}$ ), north and south poles ( $9.832 \text{ m s}^{-2}$ ), New York ( $9.801 \text{ m s}^{-2}$ ), London ( $9.812 \text{ m s}^{-2}$ ).

## COMMON SYMBOLS

A	Hamaker constant (J), area ( $\text{m}^2$ ), Helmholtz free energy
a	Atomic or molecular radius (m), headgroup area ( $\text{m}^2$ )
a, b	Constants in equations of state
$a_0$	Bohr radius (0.053 nm)
C	Interaction constant ( $\text{J m}^6$ ), aqueous solute concentration in mole fraction units ( $\text{mol dm}^{-3}/55.5$ )

$D$	Distance between two surfaces (m)
Da	Dalton unit of molecular weight (same as MW)
$E$	Electric field strength ( $V\ m^{-1}$ )
$F$	Force (N)
$G$	Gibbs free energy
$H$	Enthalpy
$I$	Ionization potential (J)
$i$	$\sqrt{-1}$
$K$	Elastic modulus ( $N\ m^{-2}$ ), spring constant ( $N\ m^{-1}$ )
$K_a$	Reaction constant, association constant ( $M^{-1}$ )
$K_d$	Dissociation constant ( $= 1/K_a$ )
$k_a$	Area compressibility modulus ( $J\ m^{-2}$ )
$k_b$	Bending modulus (J)
$L$	Latent heat ( $J\ mol^{-1}$ ), thickness of polymer brush layer (m)
$l$	Length (m), unit segment length in polymer chain (m)
$l_c$	Critical hydrocarbon chain length (m)
$M$	Concentration ( $\text{mol dm}^{-3}$ ), molecular weight, mean aggregation number
MW	Molecular weight (Da)
$m$	Mass (kg)
$n$	Refractive index, number of segments in a polymer chain
$P$	Pressure ( $N\ m^{-2}$ )
$pK$	$-\log_{10}[\text{concentration of H}^+ \text{ ions in M}]$
$Q, q$	Charge (C)
$R$	Radius (m)
$R_g$	Radius of gyration of polymer (m)
$R_F$	Flory radius of polymer (m)
$r$	Interatomic distance (m), radius (m)
$S$	Entropy
$s$	Mean distance between polymer anchoring sites (m)
$T$	Temperature (K)
$T_M, T_B$	Melting or boiling points (K or $^{\circ}\text{C}$ )
$T_c$	Lipid chain melting temperature
$u$	Dipole moment ( $C\ m$ )
$U$	Molar cohesive energy ( $J\ mol^{-1}$ ), internal energy ( $J\ mol^{-1}$ )
$V, v$	Molar volume ( $\text{m}^3$ ), volume ( $\text{m}^3$ )
$W, w$	Interaction free energy (J), pair potential (J)
$X$	Dimensionless concentration (e.g., mole fraction)
$Y$	Young's modulus ( $N\ m^{-2}$ )
$z$	Valency
$\alpha$	Polarizability ( $C^2\ m^2\ J^{-1}$ ), interaction energy parameter (J or $J\ m^{-1}$ )

$\gamma$	Surface tension ( $N\ m^{-1}$ ), surface energy ( $J\ m^{-2}$ ), $\tanh(e\psi_0/4kT) \approx \tanh[\psi_0(\text{mV})/103]$ at 298 K
$\gamma_i, \gamma_{AB}$	Interfacial energy ( $J\ m^{-2}$ )
$\Gamma$	Surface coverage (number per $\text{m}^2$ )
$\delta$	Stern layer thickness (m)
$\epsilon$	Relative permittivity, static dielectric constant
$\epsilon$	Energy ( $J$ or $J\ m^{-1}$ )
$\theta$	Angle (deg or rad), theta temperature of solvent (K)
$\kappa$	Inverse Debye length ( $\text{m}^{-1}$ )
$\lambda, \lambda_0$	Characteristic exponential decay length, wavelength (m)
$\xi$	Correlation length (m)
$\mu$	Chemical potential
$\mu^i, \mu^0$	Standard part of chemical potential due to interactions
$v, v_I$	Frequency ( $\text{s}^{-1}$ or Hz), ionization frequency ( $\text{s}^{-1}$ )
$\rho$	Number density ( $\text{m}^{-3}$ ) or mass density ( $\text{kg}\ \text{m}^{-3}$ )
$\sigma$	Atomic or molecular diameter (m)
$\tau$	surface charge density ( $C\ \text{m}^{-2}$ ), standard deviation
$\phi$	Characteristic relaxation time (s)
$\psi$	Angle (deg or rad)
$\psi_0$	Electrostatic potential (V)
$\Pi$	Electrostatic surface potential (V)
$\approx, \sim$	Approximately equal to, roughly
$>, <$	Greater than, less than
$\gtrapprox$	Slightly greater than
$\geqslant$	Greater than or equal to
$\equiv$	Equivalent to
$\propto$	Proportional to
$\Delta$	Change or difference in
$\gg, \ll$	Much greater than, less than
$\langle X \rangle$	Average or mean of $X$
$[X]$	Concentration of $X$
$\rightarrow$	Approaches
$\square$	Start or end of Worked Example

by coating the spheres with a ‘matching layer’ of surfactant, the depth of the potential well was reduced by a factor of 10 as ascertained by light scattering measurements. When asked about the thickness of the layer, Dr Chan replies that this is proprietary information.

What was the thickness of the layer?

**11.11** Are there realistic conditions for which the effective Hamaker ‘constant’ (i) increases with distance, and (ii) is higher in a medium than in free space?

**11.12** Derive the expression for the non-retarded force between two thin membranes 2 of thickness  $T$  whose surfaces are at a distance  $D$  apart in medium 1. Show that at a separation of  $D = 2.2T$  the force between them is half that of two half-spaces of 2 across 1 at the same separation  $D$ . Also show that at larger separations, when  $D \gg T$ , the non-retarded interaction energy between two sheets approaches

$$W(D) = -A_{121} T^2 / 2\pi D^4. \quad (11.42)$$

## CHAPTER 12

### ELECTROSTATIC FORCES BETWEEN SURFACES IN LIQUIDS

#### 12.1 THE CHARGING OF SURFACES IN LIQUIDS: THE ELECTRIC ‘DOUBLE LAYER’

Situations in which van der Waals forces alone determine the total interaction are restricted to a few simple systems, for example, to interactions in a vacuum or to non-polar wetting films on surfaces, both of which were discussed in Chapter 11. In more complex, and more interesting, systems long-range electrostatic forces are also involved, and the interplay between these two interactions has many important consequences.

As mentioned earlier the van der Waals force between similar particles in a medium is always attractive, so that if only van der Waals forces were operating, we might expect all dissolved particles to stick together (coagulate) immediately and precipitate out of solution as a mass of solid material. Our own bodies would be subject to the same fate if we remember that we are composed of about 75% water. Fortunately this does not happen, because particles suspended in water and any liquid of high dielectric constant are usually charged and can be prevented from coalescing by repulsive electrostatic forces. Other repulsive forces that can prevent coalescence are solvation and steric forces, described in Chapters 13 and 14. In this chapter we shall concentrate on the electrostatic forces.

The charging of a surface in a liquid can come about in two ways:

- (i) by the ionization or dissociation of surface groups (e.g., the dissociation of protons from surface carboxylic groups ( $\text{--COOH} \rightarrow \text{--COO}^- + \text{H}^+$ ), which leaves behind a negatively charged surface) and
- (ii) by the adsorption (binding) of ions from solution onto a previously uncharged surface, e.g., the binding of  $\text{Ca}^{2+}$  onto the zwitterionic headgroups of lipid bilayer surfaces, which charges the surfaces positively. Depending on the ionic conditions, even the air–water and hydrocarbon–water interfaces can become charged in this way. The adsorption of ions from solution can, of course, also occur onto oppositely charged surface sites, e.g., the adsorption

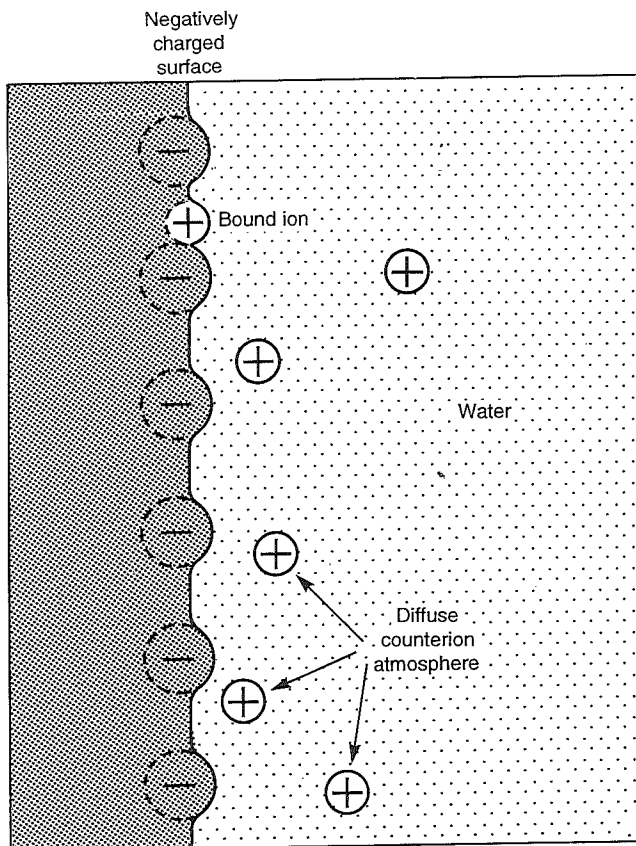


Fig. 12.1. Ions bound to a surface are not rigidly bound but can exchange with other ions in solution; their lifetime on a surface can be as short as  $10^{-9}$  s or as long as many hours.

of cationic  $\text{Ca}^{2+}$  to anionic  $\text{COO}^-$  sites vacated by  $\text{H}^+$  or  $\text{Na}^+$ . This is known as *ion exchange*.

Whatever the *charging mechanism*, the final surface charge is balanced by an equal but oppositely charged region of *counterions*, some of which are bound, usually transiently, to the surface within the so-called *Stern* or *Helmholtz layer*, while others form an atmosphere of ions in rapid thermal motion close to the surface, known as the diffuse *electric double layer* (Fig. 12.1).

Two similarly charged surfaces usually repel each other electrostatically in solution, though under certain conditions they may attract at small

separations. Zwitterionic surfaces, i.e., those characterized by surface dipoles but no net charge, also interact electrostatically with each other, though here we shall find that the force is usually attractive.

## 12.2 CHARGED SURFACES IN WATER (NO ADDED ELECTROLYTE)

In the following sections we shall consider the counterion distribution and force between two similarly charged planar surfaces in a pure liquid such as water, where (apart from  $\text{H}_3\text{O}^+$  and  $\text{OH}^-$  ions) the only ions in the solution are those that have come off the surfaces. Such systems occur when, for example, colloidal particles, clay sheets, surfactant micelles or bilayers whose surfaces contain ionizable groups interact in water, and also when thick films of water build up (condense) on an ionizable surface such as glass. But first we must consider some fundamental equations that describe the counterion distribution between two charged surfaces in solution.

## 12.3 THE POISSON–BOLTZMANN (PB) EQUATION

For the case when only counterions are present in solution, the chemical potential of any ion may be written as

$$\mu = z\psi + kT \log \rho, \quad (12.1)$$

where  $\psi$  is the electrostatic potential and  $\rho$  the number density of ions of valency  $z$  at any point  $x$  between two surfaces (Fig. 12.2). Since only differences in potential are ever physically meaningful, we may set  $\psi_0 = 0$  at the midplane ( $x = 0$ ), where also  $\rho = \rho_0$  and  $(d\psi/dx)_0 = 0$  by symmetry.

From the equilibrium requirement that the chemical potential be uniform throughout, Eq. (12.1) gives us the expected Boltzmann distribution of counterions at any point  $x$ :

$$\rho = \rho_0 e^{-ze\psi/kT}. \quad (12.2)$$

One further important fundamental equation will be required. This is the well-known *Poisson equation* for the net excess charge density at  $x$ :

$$ze\rho = -\epsilon\epsilon_0(d^2\psi/dx^2) \quad (12.3)$$

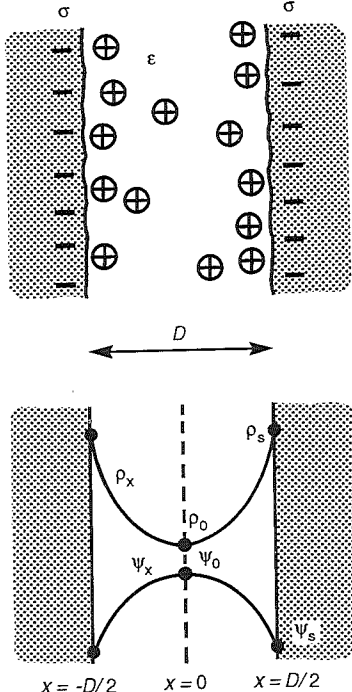


**Fig. 12.2.** Two negatively charged surfaces of surface charge density  $\sigma$  separated a distance  $D$  in water. The only ions in the space between them are the counterions that have dissociated from the surfaces. The counterion density profile  $\rho_x$  and electrostatic potential  $\psi_x$  are shown schematically in the lower part of the figure. The 'contact' values are  $\rho_s$  and  $\psi_s$ .

which when combined with the Boltzmann distribution, Eq. (12.2), gives the Poisson–Boltzmann (PB) equation:

$$\frac{d^2\psi}{dx^2} = -ze\rho/\epsilon\epsilon_0 = -(ze\rho_0/\epsilon\epsilon_0)e^{-ze\psi/kT}. \quad (12.4)$$

When solved, the PB equation gives the potential  $\psi$ , electric field  $E = \partial\psi/\partial x$ , and counterion density  $\rho$ , at any point  $x$  in the gap between the two surfaces. Let us first determine these values at the surfaces themselves. These quantities are often referred to as the *contact values*:  $\psi_s$ ,  $E_s$ ,  $\rho_s$ , etc.

#### 12.4 SURFACE CHARGE, ELECTRIC FIELD AND COUNTERION CONCENTRATION AT A SURFACE

The PB equation is a non-linear second-order differential equation, and to solve for  $\psi$  we need two *boundary conditions*, which determine the two integration constants. The first boundary condition follows from the symmetry requirement that the field must vanish at the midplane, i.e., that  $E_0 = (d\psi/dx)_0 = 0$ . The second boundary condition follows from the requirement of overall *electroneutrality*, i.e., that the total charge of the counterions in the gap must be equal (and opposite) to the charge on the surfaces. If  $\sigma$  is the surface charge density on each surface (in  $C\ m^{-2}$ ) and  $D$  is the distance between the surfaces (Fig. 12.2), then the condition of electroneutrality implies that

$$\begin{aligned} \sigma &= - \int_0^{D/2} zep \, dx = +\epsilon\epsilon_0 \int_0^{D/2} (d^2\psi/dx^2) \, dx \\ &= \epsilon\epsilon_0 (d\psi/dx)_{D/2} = \epsilon\epsilon_0 (d\psi/dx)_s = \epsilon\epsilon_0 E_s, \end{aligned}$$

i.e.

$$E_s = \sigma/\epsilon\epsilon_0. \quad (12.5)$$

Eq. (12.5) gives an important boundary condition relating the surface charge density  $\sigma$  to the electric field  $E_s$  at each surface (at  $x = \pm D/2$ ), which we may note is independent of the gap width  $D$ .



#### WORKED EXAMPLE

**Question:** Is the electric field near a charged surface in water sufficiently intense to immobilize the water molecules adjacent to it?

**Answer:** Assuming a high charge density of  $\sigma = 0.3\ C\ m^{-2}$  (which is one charge per  $0.5\ nm^2$ —typical of a fully ionized surface), the electric field at the surface, Eq. (12.5), is  $E_s = \sigma/\epsilon\epsilon_0 = 0.3/80(8.85 \times 10^{-12}) = 4.2 \times 10^8\ V\ m^{-1}$ . We may compare this to the field just outside a monovalent ion in water. Using Eq. (3.3), the field at  $r = 0.25\ nm$  from the centre of an ion is  $E_r = e/4\pi\epsilon\epsilon_0 r^2 = 2.9 \times 10^8\ V\ m^{-1}$ . Since this is comparable to the field at the charged surface, and since the fields of monovalent ions are usually not strong enough to immobilize water molecules around them (Chapters 3–5), it is unlikely that water molecules will become significantly

oriented, immobilized, or ‘bound’ to, any but the most highly charged surfaces. However, other interactions with the surface, such as H-bonding, may lead to significant effects on the local water structure.  $\square$

Turning now to the ionic distribution, there exists an important general relation between the concentrations of counterions at either surface and at the midplane. Differentiating Eq. (12.2) and then using Eq. (12.4) we obtain

$$\begin{aligned}\frac{d\rho}{dx} &= -\frac{ze\rho_0}{kT} e^{-ze\psi/kT} \left(\frac{d\psi}{dx}\right) = \frac{\varepsilon\varepsilon_0}{kT} \left(\frac{d\psi}{dx}\right) \left(\frac{d^2\psi}{dx^2}\right) \\ &= \frac{\varepsilon\varepsilon_0}{2kT} \frac{d}{dx} \left(\frac{d\psi}{dx}\right)^2,\end{aligned}\quad (12.6)$$

hence

$$\rho_x - \rho_0 = \int_0^x d\rho = \frac{\varepsilon\varepsilon_0}{2kT} \int_0^x d\left(\frac{d\psi}{dx}\right)^2 = + \frac{\varepsilon\varepsilon_0}{2kT} \left(\frac{d\psi}{dx}\right)_x^2$$

so that

$$\rho_x = \rho_0 + \frac{\varepsilon\varepsilon_0}{2kT} \left(\frac{d\psi}{dx}\right)_x^2, \quad (12.7)$$

which gives  $\rho$  at any point  $x$  in terms of  $\rho_0$  at the midplane and  $(d\psi/dx)^2$  at  $x$ . In particular at the surface,  $x = D/2$ , we obtain using Eq. (12.5) the contact value of  $\rho$

$$\rho_s = \rho_0 + \sigma^2/2\varepsilon\varepsilon_0 kT. \quad (12.8)$$

This result shows that the concentration of counterions at the surface depends only on the surface charge density  $\sigma$  and the counterion concentration at the midplane. Note that  $\rho_s$  never falls below  $\sigma^2/2\varepsilon\varepsilon_0 kT$  even for isolated surfaces, i.e., for two surfaces far apart when  $\rho_0 \rightarrow 0$ . For example, for an isolated surface in water of charge density  $\sigma = 0.2 \text{ C m}^{-2}$  (one charge per  $0.8 \text{ nm}^2$ ) at  $293 \text{ K}$

$$\begin{aligned}\rho_s &= \sigma^2/2\varepsilon\varepsilon_0 kT = (0.2)^2/2 \times 80 \times 8.85 \times 10^{-12} \times 4.04 \times 10^{-21} \\ &= 7.0 \times 10^{27} \text{ m}^{-3}\end{aligned}$$

which is about 12 M. If these surface counterions are considered to occupy

a layer of thickness  $\sim 0.2 \text{ nm}$ , the above value for  $\rho_s$  corresponds to a surface counterion density of  $(7 \times 10^{27})(0.2 \times 10^{-9}) = 1.4 \times 10^{18} \text{ ions m}^{-2}$  or one charge per  $0.7 \text{ nm}^2$ , which is about the same as the surface charge density  $\sigma$ . This is an interesting result, for it shows that regardless of the counterion distribution profile  $\rho_x$  away from a surface (Section 12.5), most of the counterions that effectively balance the surface charge are located in the first few ångströms from the surface (Jönsson *et al.*, 1980). However, for lower surface charge densities, since  $\rho_s \propto \sigma^2$ , the layer of counterions extends well beyond the surface and becomes much more diffuse (hence the term *diffuse double layer*).

## 12.5 COUNTERION CONCENTRATION PROFILE AWAY FROM A SURFACE

The above equations are quite general and are the starting point of all theoretical computations of the ionic distributions near planar charged surfaces, even when the solution contains added electrolyte (Section 12.11 onwards). To proceed further for the specific case of counterions only (Fig. 12.2) we must now solve the Poisson–Boltzmann equation, Eq. (12.4), which can be satisfied by

$$\psi = (kT/ze) \log(\cos^2 Kx) \quad (12.9)$$

or

$$e^{-ze\psi/kT} = 1/\cos^2 Kx, \quad (12.10)$$

where  $K$  is a constant given by

$$K^2 = (ze)^2 \rho_0 / 2\varepsilon\varepsilon_0 kT. \quad (12.11)$$

With this form for the potential we see that  $\psi = 0$  and  $d\psi/dx = 0$  at  $x = 0$  for all  $K$ , as required. To solve for  $K$  we differentiate Eq. (12.9) and then use Eq. (12.5) to obtain for the electric fields

at any point  $x$ :  $E_x = d\psi/dx = -(2kTK/ze) \tan Kx$ ,

at the surfaces:  $E_s = (d\psi/dx)_s = -(2kTK/ze) \tan (KD/2) = +\sigma/\varepsilon\varepsilon_0$ .

$$(12.12)$$

The counterion distribution profile

$$\rho_x = \rho_0 e^{-ze\psi/kT} = \rho_0 / \cos^2 Kx \quad (12.13)$$

is therefore known once  $K$  is determined from Eq. (12.12) in terms of  $\sigma$  and  $D$ .



### WORKED EXAMPLE

**Question:** Two charged surfaces with  $\sigma = 0.2 \text{ C m}^{-2}$  are 2 nm apart ( $D = 2 \text{ nm}$ ). Calculate the field, potential and counterion density at each surface, at 0.2 nm from each surface and at the mid-plane, assuming monovalent counterions.

**Answer:** From Eq. (12.12) we find that for  $z=1$ ,  $K = 1.3361 \times 10^9 \text{ m}^{-1}$  at 293 K. From Eq. (12.11) this means that  $\rho_0 = 0.40 \times 10^{27} \text{ m}^{-3}$ , so that at the surface  $\rho_s = \rho_0 / \cos^2(KD/2) = 7.4 \times 10^{27} \text{ m}^{-3}$ . The same result is also immediately obtainable from Eq. (12.8) since, as we have previously established,  $\sigma^2/2\epsilon\epsilon_0 kT = 7.0 \times 10^{27} \text{ m}^{-3}$ . Thus, the counterion concentration at each surface  $\rho_s$  is about 18.5 times greater than at the midplane  $\rho_0$ , which is only 1 nm away. Putting  $K = 1.3661 \times 10^9 \text{ m}^{-1}$ ,  $kT = 4.045 \times 10^{-21} \text{ J}$ ,  $\sigma = 0.2 \text{ C m}^{-2}$ ,  $\epsilon = 80$ ,  $ze = 1.602 \times 10^{-19} \text{ C}$ , and  $D = 2 \times 10^{-9} \text{ m}$  into Eqs (12.9), (12.12) and (12.13) we obtain:

	$\psi$ (mV)	$E$ ( $\text{V m}^{-1}$ )	$\rho$ ( $\text{m}^{-3}$ )
At $x = 1 \text{ nm}$ (‘contact value’ at surface)	-74	$2.8 \times 10^8$	$7.4 \times 10^{27} (12 \text{ M})$
At $x = 0.8 \text{ nm}$ (0.2 nm from surface)	-37	$1.2 \times 10^8$	$1.7 \times 10^{27} (3 \text{ M})$
At $x = 0$ (‘midplane’ value 1 nm from surface)	0	0	$0.4 \times 10^{27} (0.7 \text{ M})$

Note the unphysically steep decrease in the ion density  $\rho$  near the surface. □

Figure 12.3 shows how the counterion concentration varies with distance for the case of  $\sigma = 0.224 \text{ C m}^{-2}$ ,  $D = 21 \text{ nm}$ , as calculated on the basis of (i) the Poisson–Boltzmann equation as in the above example, and (ii) a Monte Carlo simulation of the same system. The agreement is quite good though the Monte Carlo result gives a slightly higher counterion concentration

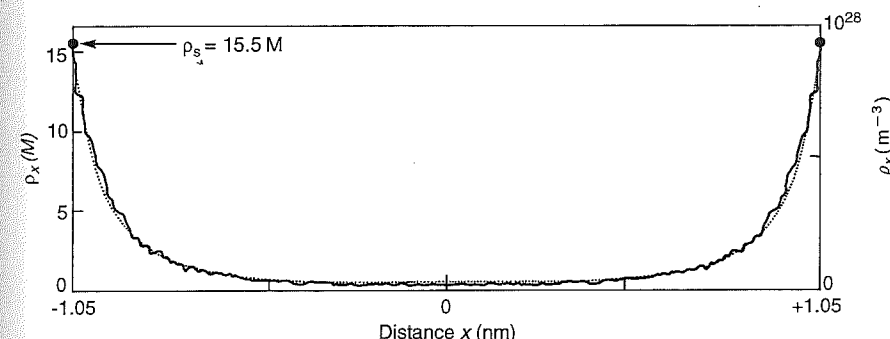
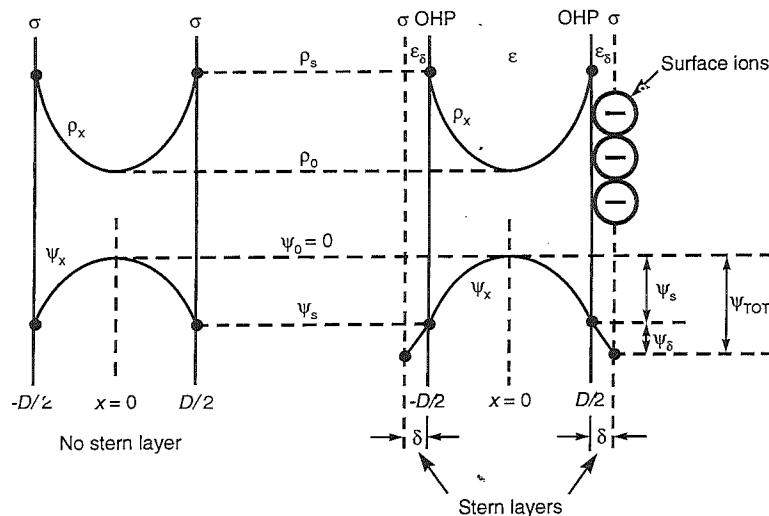


Fig. 12.3. Monovalent counterion concentration profile between two charged surfaces ( $\sigma = 0.224 \text{ C m}^{-2}$ , corresponding to one electronic charge per  $0.714 \text{ nm}^2$ ) a distance  $2.1 \text{ nm}$  apart in water. The smooth curve is obtained from the Poisson–Boltzmann equation; the other is from a Monte Carlo simulation by Jönsson *et al.* (1980).

very near the surfaces compensated by a lower concentration in the central region between the two surfaces.

### 12.6 ORIGIN OF THE IONIC DISTRIBUTION, ELECTRIC FIELD, SURFACE POTENTIAL AND PRESSURE

Before we proceed to calculate the force or pressure between two surfaces it is instructive to discuss, in qualitative terms, how the counterion distribution, potential, field and pressure between two surfaces arise. The first thing to notice is that if there were no ions between two similarly charged surfaces, there would be no electric field in the gap between them. This is because the field emanating from a planar charged surface,  $E = \sigma/2\epsilon\epsilon_0$ , is uniform away from the surface (Section 3.3). The two opposing fields emanating from the two plane parallel surfaces therefore cancel out to zero between them. Thus, when the counterions are introduced into the intervening region they do *not* experience an attractive electrostatic force towards each surface. The reason why the counterions build up at each surface is simply because of their mutual repulsion and is similar to the accumulation of mobile charges on the surface of any charged conductor. The repulsive electrostatic interaction between the counterions and their entropy of mixing alone determine their concentration profile  $\rho_x$ , the potential profile  $\psi_x$  and the field  $E_x$  between the surfaces (Jönsson *et al.*, 1980), and we may further note that in all the



**Fig. 12.4.** Stern layers of thickness  $\delta$  at each surface dividing the planes of fixed charge density  $\sigma$  from the boundary of the aqueous solution—the OHP. There is an additional linear drop in potential across the Stern layer given by Eq. (12.14) so that  $\psi_{\text{TOT}} = \psi_\delta + \psi_s$ . However, the counterion density and electrostatic potential within the aqueous region between the two OHPs at  $x = D/2$  and  $x = -D/2$ , and the pressure between the two surfaces, are independent of  $\delta$ .

theoretical derivations so far the only way the surface charge density  $\sigma$  enters into the picture is through Eq. (12.5), which is simply a statement about the total number of counterions in the gap.

Further, if the locations of the charged surface groups were not at the physical solid–liquid interface (at  $x = \pm \frac{1}{2}D$ ) but at some small distance  $\delta$  within the surface (Fig. 12.4), the ionic distribution  $\rho_x$ , potential  $\psi_x$ , field  $E_x$ , and the pressure in the medium between  $\pm \frac{1}{2}D$  and  $\pm \frac{1}{2}D + \delta$  would not change. But the potential would be different if it were measured at  $x = \pm (\frac{1}{2}D + \delta)$ . This is the origin of the so called *Stern* and *Helmholtz layers* (Verwey and Overbeek, 1948; Hiemenz, 1977) which separate the charged plane from the *Outer Helmholtz Plane* (OHP) from which the ionic atmosphere begins to obey the Poisson–Boltzmann equation. The combined thickness of the Stern and Helmholtz layers  $\delta$  is of the order of a few Ångströms and reflects the finite size of the charged surface groups and transiently bound counterions, as illustrated in Fig. 12.4. If the dielectric constant of the Stern–Helmholtz layer is uniform and equal to  $\varepsilon_\delta$  it can be modelled as a

capacitor (see Worked Example in Section 3.3) whence the additional drop in potential across the layer is given by

$$\psi_\delta = \sigma\delta/\varepsilon_\delta\varepsilon_0. \quad (12.14)$$

For example, if  $\delta = 0.2 \text{ nm}$ ,  $\sigma = 0.2 \text{ C m}^{-2}$  and  $\varepsilon_\delta = 40$ , we obtain  $\psi_\delta = 130 \text{ mV}$ , which is actually higher than the potential drop across the diffuse double layer, calculated in the previous worked example.

We now turn to the origin of the force or pressure between the two surfaces. Contrary to intuition, the origin of the repulsive force between two similarly charged surfaces in a solvent containing counterions and electrolyte ions is entropic (osmotic), not electrostatic. Indeed, the electrostatic contribution to the net force is actually attractive. Consider a surface, initially uncharged, placed in water. When the surface groups dissociate the counterions leave the surface against the attractive Coulombic force pulling them back. What maintains the diffuse double layer is the repulsive osmotic pressure between the counterions which forces them away from the surface and from each other so as to increase their configurational entropy. On bringing two such surfaces together one is therefore forcing the counterions back onto the surfaces against their preferred equilibrium state, i.e., against their osmotic repulsion, but favoured by the electrostatic interaction. The former dominates and the net force is repulsive.

To understand why the purely electrostatic part of the interaction is attractive recall that it involves an equal number of positive (counterion) and negative (surface) charges, i.e., the system is overall electrically neutral. The net Coulombic interaction between a system of charges that are overall neutral always favours their association, as we saw in the case of ionic crystals (e.g., NaCl) in Chapter 3 and dipoles in Chapter 4. This point will be further clarified in the following section.

## 12.7 THE PRESSURE BETWEEN TWO CHARGED SURFACES IN WATER: THE CONTACT VALUE THEOREM

Using Eq. (2.20) the repulsive pressure  $P$  of the counterions at any position  $x$  from the centre (Fig. 12.4) is given by  $(\partial P/\partial x)_{x,T} = \rho(\partial\mu/\partial x)_{x,T}$ , where the chemical potential  $\mu$  is given by Eq. (12.1). The change in pressure at  $x$  on bringing two plates together from infinity ( $x' = \infty$ , where  $P = 0$ ) to a

separation  $x' = D/2$  at constant temperature is therefore

$$P_x = - \int_{x' = D/2}^{x' = \infty} [ze\rho(d\psi/dx)_x dx' + kT d\rho_x]. \quad (12.15)$$

Note that in the above equation the values are computed at the *fixed* point  $x$  within the ionic solution which is not the same as the *variable* separation  $x'$  between the two surfaces. Replacing  $ze\rho$  by the Poisson equation and using the relations

$$\frac{d}{dx} \left( \frac{d\psi}{dx} \right)^2 = 2 \left( \frac{d\psi}{dx} \right) \left( \frac{d^2\psi}{dx^2} \right)$$

this becomes

$$P_x(D) - P_x(\infty) = -\frac{1}{2}\varepsilon\varepsilon_0 \left( \frac{d\psi}{dx} \right)_{x(D)}^2 + kT\rho_x(D) + \frac{1}{2}\varepsilon\varepsilon_0 \left( \frac{d\psi}{dx} \right)_{x(\infty)}^2 - kT\rho_x(\infty) \quad (12.16)$$

where the subscripts  $x$  mean that the values are calculated at  $x$  when the surfaces are at a distance  $D$  or  $\infty$  apart. In the present case, since there are no electrolyte ions in the bulk solution,  $\rho_0(\infty) = 0$ , so that by Eq. (12.7) we have  $P_x(\infty) = 0$ , as expected. The above important equation gives the pressure  $P$  at any point  $x$  between the two surfaces, and we may notice that it is split into two contributions. The first, being a square, is always negative, i.e., *attractive*. This is the electrostatic field energy contribution, discussed qualitatively in the previous section. The second term is positive and hence repulsive. This is the entropic (osmotic) contribution to the force.

At equilibrium,  $P_x(D)$  should be uniform throughout the gap, i.e., independent of  $x$ , and it is also the pressure acting on the two surfaces. To verify this we note that using Eq. (12.7) the above may be written as

$$P_x(D) = kT[\rho_0(D) - \rho_0(\infty)] \quad (12.17a)$$

or

$$P_x(D) = kT\rho_0(D) \quad \text{since here } \rho_0(\infty) = 0. \quad (12.17b)$$

which is indeed independent of  $x$  and depends only on the increased ionic concentration, or osmotic pressure, at the *midplane*,  $\rho_0(D)$ , and thus on  $\sigma$

and  $D$ . We may therefore drop the subscript  $x$  from  $P_x(D)$ . It is instructive to insert Eq. (12.8) into the above, whence we obtain

$$P(D) = kT\rho_0(D) = kT[\rho_s(D) - \sigma^2/2\varepsilon\varepsilon_0 kT],$$

that is,

$$P(D) = kT[\rho_s(D) - \rho_s(\infty)]. \quad (12.18)$$

Thus, the pressure is also given by the increase in the ion concentration at the *surfaces* as they approach each other. This important equation, known as the *contact value theorem*, is always valid so long as there is no interaction between the counterions and the surfaces, i.e., so long as there is no counterion adsorption so that the surface charge density remains constant and independent of  $D$ .

The contact value theorem is very general and applies to many other types of interactions, for example, to double-layer interactions when electrolyte ions are present in the solution, to solvation interactions where  $\rho_s(D)$  is now the surface concentration of solvent molecules (Chapter 13), to polymer-associated steric and depletion interactions where  $\rho_s(D)$  is the surface concentration of polymeric groups (Chapters 14 and 18), and to undulation, peristaltic and protrusion forces between fluid membranes (Chapter 18). In the case of overlapping double layers, the resulting force is often referred to as the *electric* or *electrostatic* double-layer repulsion or force, even though, as we have seen, the repulsion is really due to entropic confinement.

Returning to Eq. (12.17b) the pressure may also be expressed in terms of  $K$ , as given by Eq. (12.11), by

$$P = kT\rho_0 = 2\varepsilon\varepsilon_0(kT/ze)^2 K^2. \quad (12.19)$$

As an example let us apply this result to the worked example of Section 12.5 where for two surfaces with  $\sigma = 0.2 \text{ C m}^{-2}$  at  $D = 2 \text{ nm}$  apart, we found  $K = 1.336 \times 10^9 \text{ m}^{-1}$ . The repulsive pressure between them is therefore  $1.7 \times 10^6 \text{ N m}^{-2}$ , or about 1.7-atm. Note that this repulsion exceeds by far any possible van der Waals attraction at this separation; for a typical Hamaker constant of  $A \approx 10^{-20} \text{ J}$  the van der Waals attractive pressure would be only  $A/12\pi D^3 \approx 3 \times 10^4 \text{ N m}^{-2}$  or about 0.3 atm.

The above equations have been used successfully to account for the equilibrium spacings of ionic surfactant and lipid bilayers in water (Cowley *et al.*, 1978). Figure 12.5 shows experimental results obtained for the repulsive pressure between charged bilayer surfaces in water (cf. Fig. 10.6h), together with the theoretical curve based on Eq. (12.19). The agreement is very good

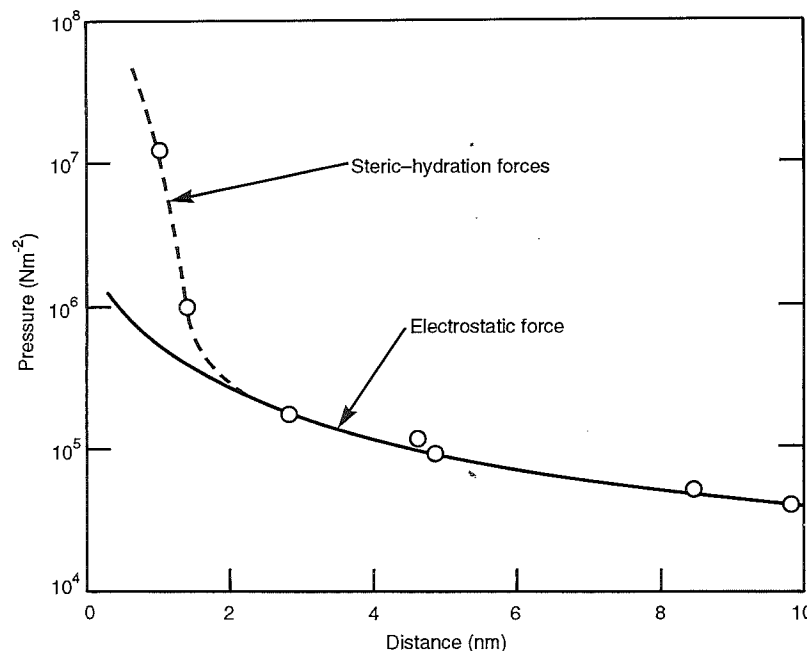


Fig. 12.5. Measured repulsive pressure between charged bilayer surfaces in water. The bilayers were composed of 90% lecithin, a neutral zwitterionic lipid, and 10% phosphatidylglycerol, a negatively charged lipid. For full ionization, the surface charge density should be one electronic charge per  $7\text{ nm}^2$ , whereas the theoretical line through the experimental points suggests one charge per  $14\text{ nm}^2$  (i.e., about 50% ionization). Below 2 nm there is an additional repulsion due to 'steric-hydration' forces. (From Cowley *et al.*, 1978, ©1978 American Chemical Society.)

down to  $D \approx 2\text{ nm}$  and shows that the effective charge density of the anionic lipid headgroups is about  $1e$  per  $14\text{ nm}^2$ . At smaller distances the measured forces are more repulsive than expected due to the steric-hydration interactions between the thermally mobile hydrophilic headgroups that characterize these surfaces (Chapters 14 and 18). Similar methods have been used to measure the repulsive electrostatic forces between biological membranes in salt solutions (Diederichs *et al.*, 1985).

Repulsive electrostatic forces also control the long-range swelling of clays in water. Most naturally occurring clays are composed of lamellar aluminosilicate sheets about 1 to 2 nm thick whose surfaces dissociate in water giving off  $\text{Na}^+$ ,  $\text{K}^+$ , and  $\text{Ca}^{2+}$  ions, and when placed in water they can swell to more than 10 times their original volume (Norrish, 1954). The

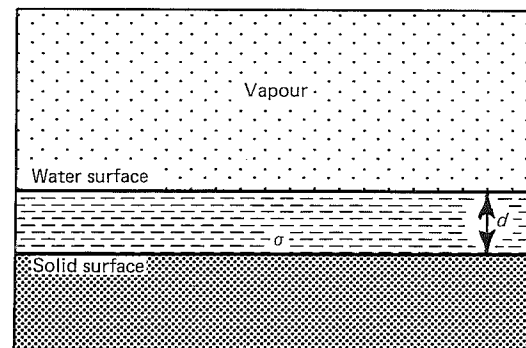


Fig. 12.6. A water film on a charged (ionizable) glass surface will tend to thicken because of the repulsive 'disjoining pressure' of the counterions in the film. If the vapour over the film is saturated, the film will grow indefinitely, but if it is unsaturated, the equilibrium thickness  $d$  will be finite as given by Eqs (12.21) and (12.22).

swelling of clays is, however, a complex matter and also involves hydration effects at surface separations below about 3 nm (van Olphen, 1977; Pashley and Quirk, 1984; Kjellander *et al.*, 1988).

In the case of charged spherical particles (e.g. latex particles) in water the long-range electrostatic repulsion between them can result in an ordered lattice of particles even when the distance between them is well in excess of their diameter (Takano and Hachisu, 1978). In such systems (cf. Fig. 10.6g) colloidal particles attempt to get as far apart from each other as possible but, being constrained within a finite volume of solution, are forced to arrange themselves into an ordered lattice (for a review see Forsyth *et al.*, 1978).

Parsegian (1966) and Jönsson and Wennerström (1981) extended the above analysis to the interactions between cylindrical and spherical structures, and the results were used to analyse the relative stability of charged surfactant aggregates which form spontaneously in water. Such micellar structures are soft and fluid-like, and they change from being spherical to cylindrical to sheet-like (bilayers) as the amount of water is reduced (see Part III).

## 12.8 LIMITATIONS OF THE POISSON–BOLTZMANN EQUATION

Like all continuum and mean-field theories the PB equation breaks down at small distances where it no longer faithfully describes the ionic distribution and forces between two surfaces. The following factors come into play at short separations:

(i) *Ion-correlation effects.* The mobile counterions in the diffuse double-layer constitute a highly polarizable layer at each interface. These two apposing ‘conducting’ layers therefore experience an attractive van der Waals force which is not included in the PB equation or the Lifshitz theory. Known as the *ion-correlation force* (Guldbrand *et al.*, 1984) this attraction becomes significant at small distances ( $< 4 \text{ nm}$ ) and it increases with the surface charge density  $\sigma$  and valency  $z$  of the counterions.

In a Monte Carlo study of the ionic density distributions, interaction energies and pressures between planar surfaces, spheres and cylinders, Wennerström *et al.* (1982) concluded that between surfaces of high charge density the attractive ion-correlation force can reduce the effective double-layer repulsion by 10–15% if the counterions are monovalent. However, with divalent counterions (e.g.,  $\text{Ca}^{2+}$ ) the ion-correlation attraction was found to exceed the double-layer repulsion—the net force becoming overall attractive—below about 2 nm, even in very dilute electrolyte solutions. Such short-range attractive ion-correlation forces have been measured between highly charged anionic bilayer surfaces in  $\text{CaCl}_2$  solutions (Marra, 1986b, c; Kjellander *et al.*, 1988, 1990), and they are believed to be responsible for the strong adhesion or non-swelling of negatively charged clay and bilayer membrane surfaces in the presence of divalent ions (Kjellander *et al.*, 1988; Khan *et al.*, 1985). Their importance in the interactions of colloidal, amphiphilic and biological surfaces have yet to be fully established.

(ii) *Finite ion size (steric) effects.* This tends to enhance the repulsion between two surfaces. The effect is analogous to the increased (osmotic) pressure of a van der Waals gas due to the finite size (excluded volume) of the gas molecules. The finite sizes of both the counterions and the co-ions contribute to the enhanced repulsion. In the case of the co-ions adsorbed on the surfaces this is simply the steric repulsion between the two overlapping Stern layers (Fig. 12.4).

(iii) *Image forces.* For counterions in water between two surfaces of lower dielectric constant the image force (Fig. 11.2) contributes an additional repulsion.

(iv) *Discreteness of surface charges.* Surface charges are discrete and not ‘smeared out’ as has been implicitly assumed. Discrete ions generally contribute an attractive force, especially if the surface charges are mobile (thereby providing an additional contribution to the ion-correlation force).

(v) *Solvation forces.* This effect has to do with the solvent rather than the ions (solute). These short-range solvation or hydration forces can be attractive, repulsive or oscillatory, and are fully described in Chapter 13.

Unfortunately, it is not possible to list the relative importance of the above effects. In some cases the short-range forces are dominated by attractive ion-correlation forces, in others by repulsive solvation forces, while in some

the forces appear to be well described by continuum theory right down to molecular contact (often because of the fortuitous cancellation of two or more opposing effects).

## 12.9 THICK WETTING FILMS

At large distances  $D$  and high surface charge densities  $\sigma$  the value of  $(KD/2)$  in Eq. (12.12) must approach  $\pi/2$  (i.e.,  $K \rightarrow \pi/D$ ). In this limit the pressure, Eq. (12.19), therefore becomes

$$P(D) = 2\epsilon\epsilon_0(\pi kT/ze)^2/D^2, \quad (12.20)$$

which is known as the *Langmuir equation*. The Langmuir equation has been used to account for the equilibrium thickness of thick wetting films of water on glass surfaces (Figs 10.6f and 12.6). Here the water–air surface replaces the midplane of Fig. 12.2, so that for a film of thickness  $d = D/2$ , we have

$$P(d) = \epsilon\epsilon_0(\pi kT/ze)^2/2d^2, \quad (12.21)$$

which is sometimes referred to as the *disjoining pressure* of a film. This repulsive pressure is entirely analogous to the repulsive van der Waals force across adsorbed liquid films, such as helium (Section 11.6), that causes them to climb up or spread on surfaces. Note, however, that both the magnitude and range of the double-layer repulsion is usually greater than the van der Waals’ ( $P \propto 1/d^2$  instead of  $P \propto 1/d^3$ ). In Section 11.6 we saw that the equilibrium thickness  $d$  of a wetting film is given by one or other of the following equivalent equations

$$P(d) = -mgH/v = (kT/v) \log(p/p_{\text{sat}}), \quad (12.22)$$

where  $H$  is the height of the film above the surface of the bulk liquid,  $v$  and  $m$  the molecular volume and mass of the solvent ( $\rho = m/v$ ), and  $p/p_{\text{sat}}$  the relative vapour pressure. Thus, if water condenses on a charged surface from undersaturated vapour, the film thickness,  $d$  will increase to infinity as  $H$  approaches zero—or, equivalently, as  $p$  approaches  $p_{\text{sat}}$ .

Langmuir (1938) first applied Eq. (12.21) to explain why the rise of water up a capillary tube is higher than expected: since the water also wets the inner surface of the capillary the effective radius is smaller than the dry radius and this leads to a higher capillary rise than expected. Derjaguin and Kusakov (1939) measured how the thickness of a water film on a quartz glass surface

decreased when an air bubble was progressively pressed on the film. The results were in rough agreement with the Langmuir equation. Read and Kitchener (1969) repeated these measurements and again found only rough agreement between theory and experiment: in the range 30–130 nm, the measured film thicknesses were 10–20 nm thicker than expected theoretically. This effect could be accounted for if the water-air interface is negatively charged so that for a given pressure  $P$  the film thickness would indeed be higher than given by Eq. (12.21), which assumes  $\sigma = 0$  and  $d\psi/dx = 0$  at that interface. More recently, Derjaguin and Churaev (1974), Pashley and Kitchener (1979), and Gee *et al.* (1990) used the vapour pressure control method to measure the equilibrium film thickness and found that for  $d < 30$  nm the films are *much* thicker than expected from Eq. (12.22), an effect that has been attributed to either repulsive hydration forces or to the presence of small amounts of soluble contaminants in the films (Pashley, 1980).

#### 12.10 LIMIT OF SMALL SEPARATIONS: CHARGE REGULATION

At small separations, as  $D \rightarrow 0$ , it is easy to verify from Eq. (12.12) that  $K^2 \rightarrow -\sigma z e / \epsilon \epsilon_0 k T D$  (note that  $\sigma$  and  $z$  must have opposite signs). Thus, the repulsive pressure  $P$  of Eq. (12.19) approaches infinity according to

$$P(D \rightarrow 0) = -2\sigma kT / zeD. \quad (12.23)$$

From Eqs (12.13) and (12.11) we further find that as  $D \rightarrow 0$  the counterion density profile between the surfaces becomes uniform and equal to

$$\rho_x \approx \rho_s \approx \rho_0 \approx -2\sigma / zeD \quad \text{at all } x. \quad (12.24)$$

Since  $-2\sigma / zeD$  is the number density of counterions in the gap this means that the limiting pressure of Eq. (12.23) is simply the osmotic pressure  $P = \rho kT$  of an ideal gas at the same density as the trapped counterions.

The infinite pressure as  $D \rightarrow 0$  implied by Eq. (12.23) is, of course, unrealistic and arises from the assumption that  $\sigma = \text{constant}$ , i.e., that the surfaces remain fully ionized even when there is a very large pressure pushing the counterions back against the surfaces. In practice when two surfaces are finally forced into molecular contact the counterions are forced to readSOR onto their original surface sites. Thus, as  $D$  approaches zero the surface charge density  $\sigma$  also falls, i.e.,  $\sigma$  becomes a function of  $D$ . This is known as *charge regulation*. The effect of charge regulation is always to reduce the

effective repulsion below that calculated on the assumption of constant surface charge and will be discussed again in Section 12.17.

Note, however, that other effects and forces can also come in at small separations (Section 12.8) and that these can be equally important in determining the forces as  $D \rightarrow 0$ .

#### 12.11 CHARGED SURFACES IN ELECTROLYTE SOLUTIONS

It is far more common for charged surfaces or particles to interact across a solution that already contains electrolyte ions (dissociated inorganic salts). In animal fluids, ions are present in concentrations of about 0.2 M, mainly NaCl or KCl with smaller amounts of MgCl<sub>2</sub> and CaCl<sub>2</sub>. The oceans have a similar relative composition of these salts but at a higher total concentration, about 0.6 M. Note that even ‘pure water’ at pH 7 is strictly an electrolyte solution containing 10<sup>-7</sup> M of H<sub>3</sub>O<sup>+</sup> and OH<sup>-</sup> ions, which cannot always be ignored. For example, for a charged isolated surface exposed to a solvent containing no added electrolyte ions (only the counterions), Eqs (12.9) and (12.12) readily show that for the isolated surface, for which  $D \rightarrow \infty$ , we obtain  $KD \rightarrow \pi$  and  $\psi_s \rightarrow \infty$ . As we shall see, this unrealistic situation is removed as soon as the bulk solvent contains even the minutest concentration of electrolyte ions.

The existence of a bulk ‘reservoir’ of electrolyte ions has a profound effect not only on the electrostatic potential but also on the force between charged surfaces, and in the rest of this chapter we shall consider this interaction as well as the total interaction potential when the attractive van der Waals force is added. But to understand the double-layer interaction between two surfaces it is necessary first to understand the ionic distribution adjacent to an isolated surface in contact with an electrolyte solution. Consider an isolated surface, or two surfaces far apart, in an aqueous electrolyte (Fig. 12.7). For convenience, we shall put  $x = 0$  at the surface rather than at the midplane. Now, all the fundamental equations derived in the previous sections are applicable to solutions containing different types of ions  $i$  (of valency  $\pm z_i$ ) so long as this is taken into account by expressing the net charge density at any point  $x$  as  $\sum_i z_i e \rho_{xi}$  and the total ionic concentration (number density) as  $\sum_i \rho_{xi}$ . Thus, Eq. (12.2) for the Boltzmann distribution of ions  $i$  at  $x$  now becomes

$$\rho_{xi} = \rho_{\infty i} e^{-z_i e \psi_x / kT} \quad (12.25)$$

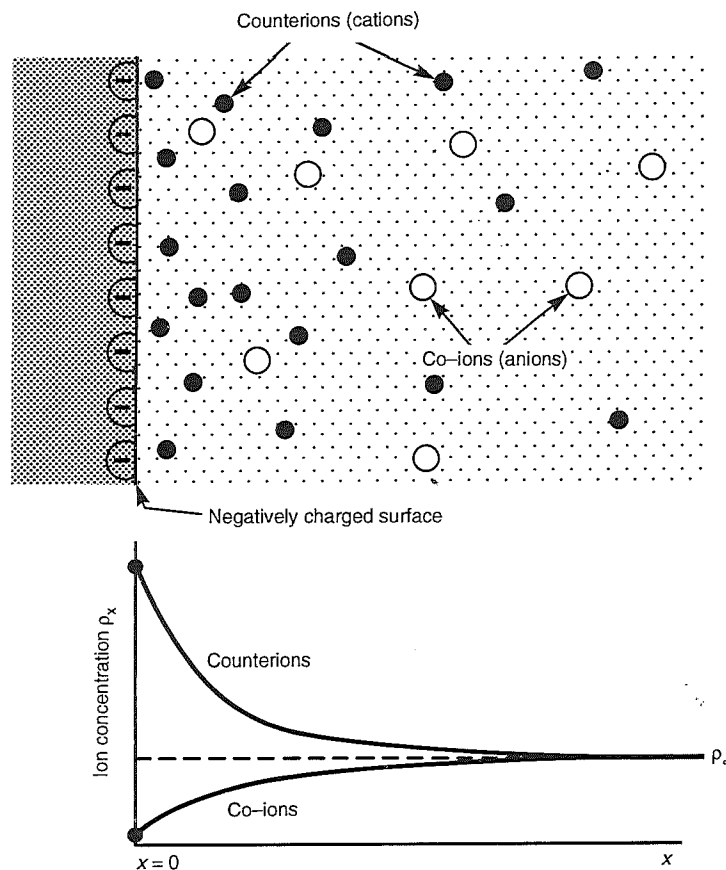


**Fig. 12.7.** Near a charged surface there is an accumulation of counterions (ions of opposite charge to the surface charge) and a depletion of co-ions, shown graphically below for a 1:1 electrolyte, where  $\rho_\infty$  is the electrolyte concentration in the bulk or 'reservoir' at  $x = \infty$ .

while at the surface, at  $x = 0$ , the contact values of  $\rho$  and  $\psi$  are related by

$$\rho_{0i} = \rho_\infty e^{-z_i e \psi_0 / kT} \quad (12.26)$$

where  $\rho_{\infty i}$  is the ionic concentration of ions  $i$  in the bulk (at  $x = \infty$ ) where  $\psi_\infty = 0$ . For example, if we have a solution containing  $\text{H}^+ \text{OH}^- +$

$\text{Na}^+ \text{Cl}^- + \text{Ca}^{2+} \text{Cl}_2^-$ , etc., we may write

$$\begin{aligned} [\text{H}^+]_x &= [\text{H}^+]_\infty e^{-e\psi_x/kT}, & [\text{H}^+]_0 &= [\text{H}^+]_\infty e^{-e\psi_0/kT}, \\ [\text{Na}^+]_x &= [\text{Na}^+]_\infty e^{-e\psi_x/kT}, & [\text{Na}^+]_0 &= [\text{Na}^+]_\infty e^{-e\psi_0/kT}, \\ [\text{Ca}^{2+}]_x &= [\text{Ca}^{2+}]_\infty e^{-2e\psi_x/kT}, & [\text{Ca}^{2+}]_0 &= [\text{Ca}^{2+}]_\infty e^{-2e\psi_0/kT}, \\ [\text{Cl}^-]_x &= [\text{Cl}^-]_\infty e^{+e\psi_x/kT}, & [\text{Cl}^-]_0 &= [\text{Cl}^-]_\infty e^{+e\psi_0/kT}, \end{aligned} \quad (12.27)$$

where  $[\text{Na}^+]$ , etc., are expressed in some convenient concentration unit such as M ( $1 \text{ M} = 1 \text{ mol dm}^{-3}$  and corresponds to a number density of  $\rho = 6.022 \times 10^{26} \text{ m}^{-3}$ ).

## 12.12 THE GRAHAME EQUATION

Let us now find the total concentration of ions at an isolated surface of charge density  $\sigma$ . From Eq. (12.8) this is immediately given by

$$\sum_i \rho_{0i} = \sum_i \rho_{\infty i} + \sigma^2 / 2\epsilon\epsilon_0 kT \quad (\text{in number per m}^3). \quad (12.28)$$

Thus, for  $\sigma = 0.2 \text{ C m}^{-2}$  (corresponding to one electronic charge per  $0.8 \text{ nm}^2$  or  $80 \text{ \AA}^2$ ) at  $25^\circ\text{C}$ , we find  $\sigma^2 / 2\epsilon\epsilon_0 kT = 7.0 \times 10^{27} \text{ m}^{-3} = 11.64 \text{ M}$ . For a 1:1 electrolyte such as  $\text{NaCl}$ , the surface concentration of ions in this case is

$$\begin{aligned} [\text{Na}^+]_0 + [\text{Cl}^-]_0 &= 11.64 + [\text{Na}^+]_\infty + [\text{Cl}^-]_\infty = 11.64 + 2[\text{Na}^+]_\infty \\ &= 11.64 + 2[\text{NaCl}], \end{aligned} \quad (12.29)$$

while for a 2:1 electrolyte such as  $\text{CaCl}_2$ ,

$$\begin{aligned} [\text{Ca}^{2+}]_0 + [\text{Cl}^-]_0 &= 11.64 + [\text{Ca}^{2+}]_\infty + [\text{Cl}^-]_\infty = 11.64 + 3[\text{Ca}^{2+}]_\infty \\ &= 11.64 + 3[\text{CaCl}_2], \end{aligned}$$

where  $[\text{NaCl}]$  and  $[\text{CaCl}_2]$  are the bulk molar concentrations of the salts. The ions at the surface are, of course, mainly the counterions (e.g.,  $\text{Na}^+$  or  $\text{Ca}^{2+}$  at a negatively charged surface) and their excess concentration at the surface over that in the bulk is seen to be

- (i) dependent solely on the surface charge density  $\sigma$  (i.e., *independent* of the bulk electrolyte concentration), and  
(ii) of magnitude sufficient to balance much of the surface charge (cf. Sections 12.4 and 12.14).

We may now find the relation between the surface charge density  $\sigma$  and the surface potential  $\psi_0$ . Incorporating Eq. (12.26) into Eq. (12.28) we obtain for the case of a mixed NaCl + CaCl<sub>2</sub> electrolyte:

$$\begin{aligned}\sigma^2 &= 2\epsilon\epsilon_0 kT \left( \sum_i \rho_{0i} - \sum_i \rho_{\infty i} \right) \\ &= 2\epsilon\epsilon_0 kT \{ [\text{Na}^+]_\infty e^{-e\psi_0/kT} + [\text{Ca}^{2+}]_\infty e^{-2e\psi_0/kT} + [\text{Cl}^-]_\infty e^{+e\psi_0/kT} \\ &\quad - [\text{Na}^+]_\infty - [\text{Ca}^{2+}]_\infty - [\text{Cl}^-]_\infty \}.\end{aligned}$$

On further noting that  $[\text{Cl}^-]_\infty = [\text{Na}^+]_\infty + 2[\text{Ca}^{2+}]_\infty$  the above becomes

$$\begin{aligned}\sigma^2 &= 2\epsilon\epsilon_0 kT \{ [\text{Na}^+]_\infty (e^{-e\psi_0/kT} + e^{+e\psi_0/kT} - 2) \\ &\quad + [\text{Ca}^{2+}]_\infty (e^{-2e\psi_0/kT} + 2e^{+e\psi_0/kT} - 3) \},\end{aligned}$$

so that finally

$$\begin{aligned}\sigma &= \sqrt{8\epsilon\epsilon_0 kT} \sin h(e\psi_0/2kT) \{ [\text{Na}^+]_\infty + [\text{Ca}^{2+}]_\infty (2 + e^{-e\psi_0/kT}) \}^{1/2} \\ &= 0.117 \sin h(\psi_0/51.4) \{ [\text{NaCl}] + [\text{CaCl}_2] (2 + e^{-\psi_0/25.7}) \}^{1/2} \quad (12.30)\end{aligned}$$

at 25°C, where the concentrations  $[\text{NaCl}] = [\text{Na}^+]_\infty$  and  $[\text{CaCl}_2] = [\text{Ca}^{2+}]_\infty$  are in M,  $\psi_0$  in mV, and  $\sigma$  in C m<sup>-2</sup> (1 C m<sup>-2</sup> corresponds to one electronic charge per 0.16 nm<sup>2</sup> or 16 Å<sup>2</sup>). Eq. (12.30) allows us to calculate  $\psi_0$  once  $\sigma$  is known, from which the individual ionic concentrations at each surface  $\rho_{0i}$  can be obtained using Eqs (12.26) or (12.27). We shall now consider some implications of this important equation, known as the *Grahame equation*.

### 12.13 SURFACE CHARGE AND POTENTIAL IN THE PRESENCE OF MONOVALENT IONS

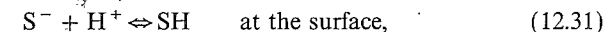
For an aqueous 1:1 electrolyte solution such as NaCl against a negatively charged surface of  $\sigma = -0.2 \text{ C m}^{-2}$ , we obtain the potentials shown in the middle column of Table 12.1. Note that for no electrolyte we obtain an

TABLE 12.1 Variation of surface potential with aqueous electrolyte concentration for a planar surface of charge density  $-0.2 \text{ C m}^{-2}$  as deduced from the Grahame equation, Eq. (12.30)

1:1 Electrolyte concentration (M)	Pure 1:1 electrolyte solution	Bulk solution also contains $3 \times 10^{-3} \text{ M}$ 2:1 electrolyte	$\psi_0$ (mV)
0 (hypothetical)	$-\infty$		-106
$10^{-7}$ (pure water)	-477		-106
$10^{-4}$	-300		-106
$10^{-3}$	-241		-106
$10^{-2}$	-181		-105
$10^{-1}$	-123		-100
1	-67		-66

infinite potential which is unrealistic; a pure liquid such as water will always contain *some* dissociated ions. It is for this reason that we did not consider an isolated surface in the absence of bulk electrolyte ions in Section 12.5. From Table 12.1 we find that at constant surface charge density the surface potential falls progressively as the electrolyte concentration rises. From the tabulated values of  $\psi_0$  we can determine the ionic concentrations at the surface using Eq. (12.27). For example, in  $10^{-7} \text{ M}$  1:1 electrolyte, where  $\psi_0 \approx -477.1 \text{ mV}$ , we obtain  $10^{-7} \times e^{+477.1/25.69} = 11.64 \text{ M}$  for the counterions, and  $10^{-7} \times e^{-477.1/25.69} \approx 10^{-15} \text{ M}$  for the co-ions. In 1 M, where  $\psi_0 = -67.0 \text{ mV}$ , we obtain 13.57 M and 0.07 M for the counterions and co-ions, respectively, which total 13.64 M. As expected, the total concentration of all the ions at the surface agrees exactly with that given by Eq. (12.29).

In most cases neither  $\sigma$  nor  $\psi_0$  remains constant as the solution conditions change. This is because ionizable surface sites are rarely fully dissociated but are partially neutralized by the binding of specific ions from the solution. Such ions are often referred to as *exchangeable* ions, in contrast to those *inert* ions that do not bind to the surface. For example, if only protons can bind to a negatively charged surface, the equilibrium condition at the surface is given by the familiar *mass action equation* (Payens, 1955). Thus, for the reaction



we may express the proton concentration at the surface as  $[\text{H}^+]_0$ , the concentration or surface density of negative (dissociated) surface sites as  $[\text{S}^-]_0$ , and the density of neutral (undissociated) sites as  $[\text{SH}]_0$ .  $[\text{S}^-]_0$  is

related to  $\sigma$  via  $\sigma = -e[S^-]_0$ . The surface dissociation constant  $K_d$  for the above 'reaction' is defined by

$$K_d = \frac{[S^-]_0[H^+]_0}{[SH]_0} \quad (12.32)$$

$$= \frac{\sigma_0 \alpha}{\sigma_0(1-\alpha)} [H^+]_0 = \frac{\alpha}{(1-\alpha)} [H^+]_\infty e^{-e\psi_0/kT}. \quad (12.33)$$

where  $\sigma_0$  is the maximum possible charge density (i.e., if all the sites were dissociated) and  $\alpha$  is the fraction of sites actually dissociated. Thus, if half the sites are dissociated at  $[H^+]_0 = 10^{-4}$  M, we have  $K_d = [H^+]_0 = 10^{-4}$  M, which may be quoted in pK units ( $pK = -\log_{10}[H^+]_0 = 4.0$  in this case). Some people prefer to describe reactions at surfaces in terms of an association or reaction constant,  $K_a$ , defined by  $K_a = 1/K_d$ .

For a mixed 1:1 electrolyte of NaCl + HCl, Eq. (12.33) can be combined with the Grahame equation to give

$$\begin{aligned} \sigma &= \sigma_0 \alpha = \sigma_0 K_d / (K_d + [HCl]) e^{-\psi_0/25.7} \\ &= 0.117 \sin h(\psi_0/51.4) \sqrt{[NaCl] + [HCl]}, \end{aligned} \quad (12.34)$$

in which both  $\sigma$  and  $\psi_0$  can now be totally determined in terms of the maximum charge density  $\sigma_0$  and dissociation constant  $K_d$  (assuming that there is no binding of  $Na^+$  ions). It is clear from the above that if  $K_d$  is very large (high surface charge, weak binding of protons) then  $\sigma \approx \sigma_0 \approx$  constant, and we obtain the earlier result for the case of fixed surface charge density. However, if  $K_d$  takes on a more typical value, the effect can be quite dramatic. For example, if  $K_d = 10^{-4}$  M, then for a surface of  $\sigma_0 = -0.2$  Cm<sup>-2</sup> in a 0.1 M NaCl bulk solution at pH 7 we find  $\psi_0 = -118$  mV and  $\alpha = 0.91$ , i.e., the protons have neutralized 9% of the surface site, and  $\psi_0$  is not very different from the value in the absence of protons (see Table 12.1). But at pH 5 we obtain  $\psi_0 = -73$  mV and  $\alpha = 0.36$ , i.e., only 36% of the sites now remain dissociated even though the bulk concentration of HCl is a mere 0.01% of the NaCl concentration. Under such conditions the proton is referred to as a potential determining ion. Thus, both  $\psi_0$  and  $\sigma$  will vary as the salt concentration or pH is changed, but the surface will always remain negatively charged.

More generally, a surface may contain both anionic (e.g., acidic) and cationic (e.g., basic) groups to which various cations and anions can bind. Such surfaces are known as *amphoteric*, and the competitive adsorption of ions to them can be analysed by assigning a binding constant to each ion

type, and then incorporating these into the Grahame equation (Healy and White, 1978; Chan *et al.*, 1980a). The charge density of amphoteric surfaces (e.g., protein surfaces) can be negative or positive depending on the electrolyte conditions. At the *isoelectric point* (iep) or *point of zero charge* (pzc) there are as many negative charges as positive charges so that the mean surface charge density is zero ( $\sigma = 0$ ), though it is well to remember that there may still be patches of high local charge density.

#### 12.14 EFFECT OF DIVALENT IONS

The presence of divalent cations has a dramatic effect on the surface potential and counterion distribution at a negatively charged surface. For example, if all the NaCl solutions of Table 12.1 also contain  $3 \times 10^{-3}$  M CaCl<sub>2</sub>, the Grahame equation gives the potentials shown in the last column. We see that even at constant surface charge density, relatively small amounts of divalent ions substantially lower the magnitude of  $\psi_0$ , in fact, about 100 times more effectively than increasing the concentration of monovalent salt. Indeed,  $\psi_0$  is determined solely by the divalent cations once their concentration is greater than about 3% of the monovalent ion concentration, and for 2:1 electrolyte concentrations above a few mM, typical surface potentials are well below -100 mV irrespective of the 1:1 electrolyte concentration.

Further, even when the bulk concentration of Ca<sup>2+</sup> is much smaller than that of Na<sup>+</sup> the surface may have a much higher local concentration of Ca<sup>2+</sup>. For example, in 100 mM NaCl + 3 mM CaCl<sub>2</sub> where  $\psi_0 = -100$  mV (Table 12.1) the concentration of Ca<sup>2+</sup> at the surface is  $[Ca^{2+}]_0 \approx 3 \times 10^{-3} e^{+200/25.7} \approx 7$  M compared to  $[Na^+]_0 \approx 0.1 e^{+100/25.7} \approx 5$  M.

At such high surface concentrations (of *doubly* charged ions) divalent ions often bind chemically to negative surface sites, thereby lowering  $\sigma$  and reducing  $\psi_0$  even further, and it is not unusual for surfaces to be completely neutralized ( $\sigma \rightarrow 0, \psi_0 \rightarrow 0$ ) in the presence of mM amounts of Ca<sup>2+</sup>. In the case of trivalent ions such as La<sup>3+</sup>, bulk concentrations in excess of  $10^{-5}$  M can neutralize a negatively charged surface and even lead to *charge reversal*, wherein the cations continue to adsorb onto a surface that is already net positively charged (see Problem 3.2).

As in the case of monovalent ion binding, the effect of divalent ion binding can be dealt with quantitatively by incorporating the appropriate binding constants into the Grahame equation (Healy and White, 1978; McLaughlin *et al.*, 1981), and when many different ionic species (e.g., Ca<sup>2+</sup>, H<sup>+</sup>) compete for binding sites the variation of  $\psi_0$  and  $\sigma$  with electrolyte concentration and pH can be quite complex. In most cases ion binding tends to lower both  $\sigma$

and  $\psi_0$  as the concentrations of these ions increase, and we may anticipate that such effects lead to a substantial reduction in the repulsive double-layer forces between surfaces.

### 12.15 THE DEBYE LENGTH

For low potentials, below about 25 mV, the Grahame equation simplifies to

$$\sigma = \epsilon\epsilon_0\kappa\psi_0, \quad (12.35)$$

where

$$\kappa = \left( \sum_i \rho_{\infty i} e^2 z_i^2 / \epsilon\epsilon_0 kT \right)^{1/2} \text{ m}^{-1}. \quad (12.36)$$

Thus, the potential becomes proportional to the surface charge density. Equation (12.35) is the same as Eq. (12.14) for a capacitor whose two plates are separated by a distance  $1/\kappa$ , have charge densities  $\pm\sigma$ , and potential difference  $\psi_0$ . This analogy with a charged capacitor gave rise to the name *diffuse electric double layer* for describing the ionic atmosphere near a charged surface, whose characteristic length or ‘thickness’ is known as the Debye length,  $1/\kappa$ .

The magnitude of the Debye length depends solely on the properties of the liquid and not on any property of the surface such as its charge or potential. At 25°C the Debye length of aqueous solutions is

$$1/\kappa = \begin{cases} 0.304/\sqrt{[\text{NaCl}]} \text{ nm} & \text{for 1:1 electrolytes (e.g., NaCl)} \\ 0.176/\sqrt{[\text{CaCl}_2]} \text{ nm} & \text{for 2:1 and 1:2 electrolytes} \\ & \text{(e.g., CaCl}_2 \text{ and Na}_2\text{SO}_4\text{)} \\ 0.152/\sqrt{[\text{MgSO}_4]} \text{ nm} & \text{for 2:2 electrolytes (e.g., MgSO}_4\text{)} \end{cases} \quad (12.37)$$

For example, for NaCl solution,  $1/\kappa = 30.4 \text{ nm}$  at  $10^{-4} \text{ M}$ ,  $9.6 \text{ nm}$  at  $1 \text{ mM}$ ,  $0.96 \text{ nm}$  at  $0.1 \text{ M}$ , and  $0.3 \text{ nm}$  at  $1 \text{ M}$ . In totally pure water at pH 7, the Debye length is  $960 \text{ nm}$ , or about  $1 \mu\text{m}$ .

### 12.16 VARIATION OF POTENTIAL AND IONIC CONCENTRATIONS AWAY FROM A CHARGED SURFACE

The potential gradient at any distance  $x$  from an isolated surface is given by Eq. (12.7):

$$\sum_i \rho_{xi} = \sum_i \rho_{\infty i} + \frac{\epsilon\epsilon_0}{2kT} \left( \frac{d\psi}{dx} \right)_x^2. \quad (12.38)$$

For a 1:1 electrolyte this gives

$$d\psi/dx = \sqrt{8kT\rho_{\infty i}/\epsilon\epsilon_0} \sinh(e\psi_x/2kT),$$

which may be readily integrated using the integral  $\int \cosh X dX = \log \tanh(X/2)$  to yield

$$\psi_x = \frac{2kT}{e} \log \left[ \frac{1 + \gamma e^{-\kappa x}}{1 - \gamma e^{-\kappa x}} \right] \approx \frac{4kT}{e} \gamma e^{-\kappa x}, \quad (12.39)$$

where

$$\gamma = \tan h(e\psi_0/4kT) \approx \tan h[\psi_0(mV)/103]. \quad (12.40)$$

This is known as the *Gouy–Chapman theory*. For high potentials  $\gamma \rightarrow 1$ , while for low potentials, Eq. (12.39) reduces to the so-called *Debye–Hückel* equation

$$\psi_x \approx \psi_0 e^{-\kappa x}, \quad (12.41)$$

where again the Debye length  $1/\kappa$  appears as the characteristic decay length of the potential (see Verwey and Overbeek, 1948, and Hiemenz, 1977, for a fuller discussion of the Gouy–Chapman and Debye–Hückel theories).

The above equations apply to *symmetrical* 1:1 electrolytes, such as NaCl. Equations that apply to *asymmetrical* electrolytes, e.g., 2:1 and 1:2 electrolytes such as CaCl<sub>2</sub>, have been derived by Grahame (1953). These are more complicated than Eq. (12.39) but for low  $\psi_0$  they all reduce to  $\psi_x = \psi_0 e^{-\kappa x}$ .

We now have all the equations needed for computing the ionic distributions away from a charged surface. For a 1:1 electrolyte, this is given by inserting Eq. (12.39) into Eq. (12.25) or (12.27). Figure 12.8 shows the variation of  $\psi_x$  and  $\rho_x$  for a 0.1 M 1:1 electrolyte, together with a Monte Carlo simulation for comparison. Note how the counterion density approaches the bulk value much faster than would be indicated by the Debye length. Indeed, for such

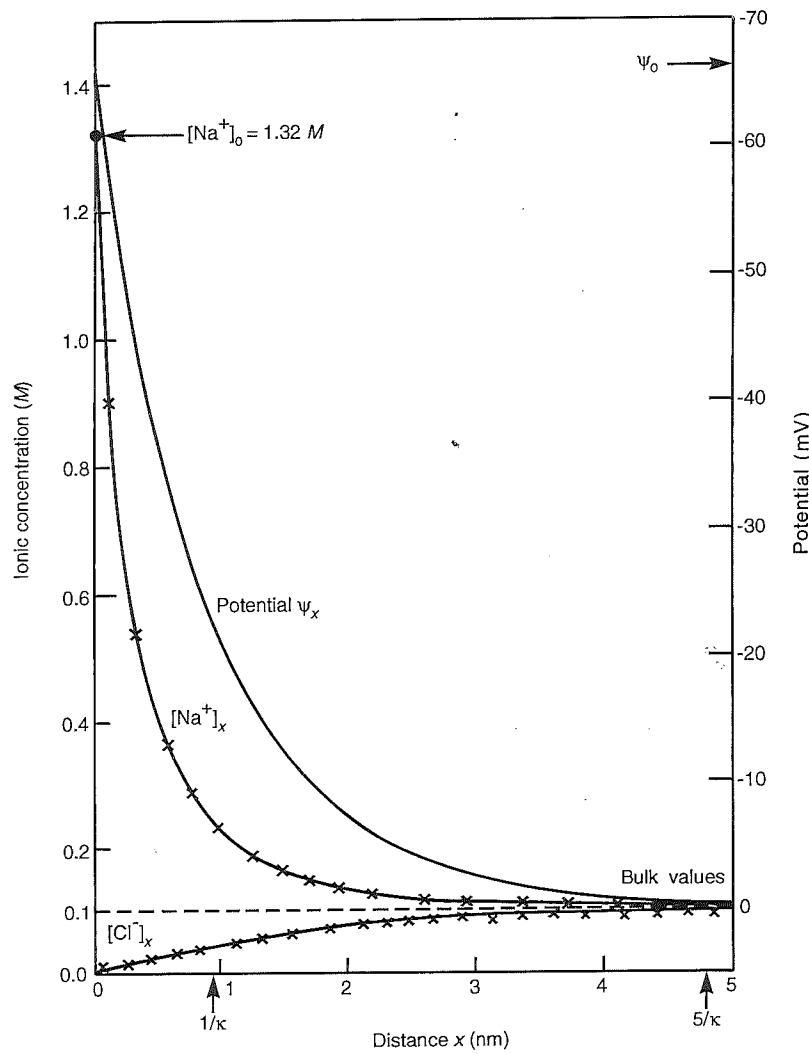


**Fig. 12.8.** Potential and ionic density profiles for a 0.1 M monovalent electrolyte such as NaCl near a surface of charge density  $\sigma = -0.0621 \text{ C m}^{-2}$  (about one electronic charge per  $2.6 \text{ nm}^2$ ), calculated from Eqs (12.39) and (12.25) with  $\psi_0 = -66.2 \text{ mV}$  obtained from the Grahame equation. The crosses are the Monte Carlo results of Torrie and Valleau (1979).

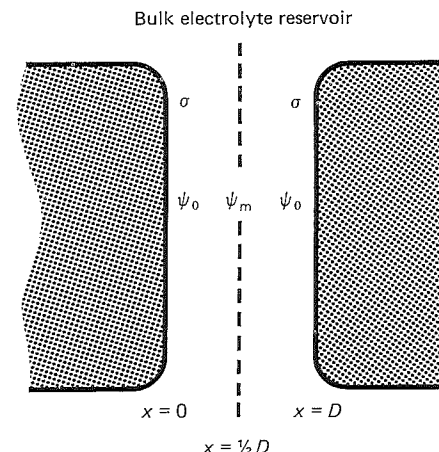


**Fig. 12.9.**

a high surface charge density and potential the counterion distribution very near the surface is largely independent of the bulk electrolyte concentration, and it is left as an exercise for the reader to verify that even in  $10^{-4} \text{ M}$  the counterion profile over the first few Ångstroms is not much different from that in 0.1 M (so long as  $\sigma$  remains the same).

### 12.17 THE ELECTROSTATIC DOUBLE-LAYER INTERACTION BETWEEN CHARGED SURFACES IN ELECTROLYTE

The interaction pressure between two identically charged surfaces in an electrolyte solution (Fig. 12.9) can be derived quite simply as follows. First, from Section 12.7 we note that at any point  $x$  the pressure  $P_x(D)$  is given by

$$P_x(D) - P_x(\infty) = -\frac{1}{2} \varepsilon \varepsilon_0 \left[ \left( \frac{d\psi}{dx} \right)_{x(D)}^2 - \left( \frac{d\psi}{dx} \right)_{x(\infty)}^2 \right] + kT \left[ \sum_i \rho_{xi}(D) - \sum_i \rho_{xi}(\infty) \right]. \quad (12.42)$$

Second, from Eq. (12.7) we have

$$\sum_i \rho_{xi} = \sum_i \rho_{mi} + \frac{\varepsilon \varepsilon_0}{2kT} \left( \frac{d\psi}{dx} \right)_x^2 \quad (12.43)$$

for any  $D$  including  $D = \infty$ , where  $\Sigma\rho_{mi}$  is the total ionic concentration at the midplane, at  $x = \frac{1}{2}D$ . Incorporating Eq. (12.43) into Eq. (12.42), and again putting  $P_x(D = \infty) = 0$ , yields

$$P_x(D) = kT \left[ \sum_i \rho_{mi}(D) - \sum_i \rho_{mi}(\infty) \right] \quad (12.44)$$

which as before is the uniform pressure across the gap (independent of position  $x$ ) acting on the electrolyte ions and on the surfaces. The above result is essentially the same as Eq. (12.17) and shows that  $P$  is simply the excess osmotic pressure of the ions in the midplane over the bulk pressure. Since  $\Sigma\rho_{mi}(\infty)$  is known from the bulk electrolyte concentration the problem reduces to finding the midplane concentration of ions  $\rho_{mi}(D)$  when  $D$  is finite, and it is here that certain assumptions have to be made to obtain an analytic result (Verwey and Overbeek, 1948). For a 1:1 electrolyte such as NaCl, Eq. (12.44) may be written as

$$P = kT\rho_\infty [(e^{-e\psi_m/kT} - 1) + (e^{+e\psi_m/kT} - 1)] \approx e^2\psi_m^2\rho_\infty/kT, \quad (12.45)$$

cations	anions
---------	--------

which assumes that the midplane potential  $\psi_m$  (not the surface potential  $\psi_0$ ) is small. If we further assume that  $\psi_m$  is simply the sum of the potentials from each surface at  $x = \frac{1}{2}D$  as previously derived for an isolated surface, then Eq. (12.39) gives  $\psi_m \approx (8kT\gamma/e)e^{-\kappa D/2}$ . Inserting this into Eq. (12.45) gives the final result for the repulsive pressure between two planar surfaces:

$$P = 64kT\rho_\infty\gamma^2 e^{-\kappa D} = (1.59 \times 10^8)[\text{NaCl}]\gamma^2 e^{-\kappa D} \text{ N m}^{-2}, \quad (12.46)$$

where we note that  $\gamma = \tan h(ze\psi_0/4kT)$  can never exceed unity. The above equation is known as the *weak overlap approximation* for the interaction between two similar surfaces at constant potential. See Problem 12.3 for the case of two surfaces with unequal surface potentials.

The interaction free energy per unit area corresponding to the above pressure is obtained by a simple integration with respect to  $D$ , and gives

$$\begin{aligned} W &= (64kT\rho_\infty\gamma^2/\kappa)e^{-\kappa D} \\ &= 0.0482[\text{NaCl}]^{1/2} \tan h^2[\psi_0(mV)/103]e^{-\kappa D} \text{ J m}^{-2} \quad (\text{for } z = 1) \\ &= 0.0211[\text{CaCl}_2]^{1/2} \tan h^2[2\psi_0(mV)/103]e^{-\kappa D} \text{ J m}^{-2} \quad (\text{for } z = 2) \end{aligned} \quad (12.47)$$

where in the above equations the concentrations  $[\text{NaCl}]$  and  $[\text{CaCl}_2]$  are in M and the values are for aqueous solutions at 298 K.

Using the Derjaguin approximation, Eq. (10.18), we may immediately write the expression for the force  $F$  between two spheres of radius  $R$  as  $F = \pi RW$ , from which the interaction free energy is obtained by a further integration:

$$W = (64\pi kTR\rho_\infty\gamma^2/\kappa^2)e^{-\kappa D} = 4.61 \times 10^{-11}R\gamma^2 e^{-\kappa D} \text{ J} \quad (\text{for } z = 1). \quad (12.48)$$

We see therefore that the double-layer interaction between surfaces or particles decays exponentially with distance. The characteristic decay length is the Debye length.

At low surface potentials, below about 25 mV, all the above equations simplify to the following. For two planar surfaces,

$$P \approx 2\epsilon\epsilon_0\kappa^2\psi_0^2 e^{-\kappa D} = 2\sigma^2 e^{-\kappa D}/\epsilon\epsilon_0 \quad (\text{per unit area}) \quad (12.49)$$

and

$$W \approx 2\epsilon\epsilon_0\kappa\psi_0^2 e^{-\kappa D} = 2\sigma^2 e^{-\kappa D}/\kappa\epsilon\epsilon_0 \quad (\text{per unit area}), \quad (12.50)$$

while for two spheres of radius  $R$ ,

$$F \approx 2\pi R\epsilon\epsilon_0\kappa\psi_0^2 e^{-\kappa D} = 2\pi R\sigma^2 e^{-\kappa D}/\kappa\epsilon\epsilon_0 \quad (12.51)$$

and

$$W \approx 2\pi R\epsilon\epsilon_0\psi_0^2 e^{-\kappa D} = 2\pi R\sigma^2 e^{-\kappa D}/\kappa^2\epsilon\epsilon_0. \quad (12.52)$$

In the above  $\psi_0$  and  $\sigma$  are related by  $\sigma = \epsilon\epsilon_0\kappa\psi_0$ , which, as we have seen, is valid for low potentials. These four equations are quite useful because they are valid for all electrolytes, whether 1:1, 2:1, 2:2, 3:1, or even mixtures, so long as the appropriate Debye lengths are used as given by Eqs (12.36) and (12.37). Thus, they are particularly suitable when divalent ions are present since the surface charge and potential is often low due to ion binding.

All the expressions so far derived for the interactions of two double layers are accurate only for surface separations beyond about one Debye length. At smaller separations one must resort to numerical solutions of the Poisson-Boltzmann equation to obtain the exact interaction potential (Verwey and Overbeek, 1948; Honig and Mul, 1971) for which there are no simple expressions. In addition there is the question of charge regulation at small separations, i.e., does the surface charge density remain constant as

two surfaces come close together, or do some of the counterions bind to the surfaces thereby reducing  $\sigma$ . This affects the form of the interaction potential. At large distances, beyond  $1/\kappa$ , the question does not arise, and the interaction pressures and energies are well described by Eqs (12.46)–(12.48), where  $\psi_0$  and  $\sigma$  are the values appropriate for the isolated surfaces (at  $D = \infty$ ). But at progressively smaller separations, as the counterion concentration at each surface increases, specific ion binding can occur as discussed earlier.

If there is no binding, the surface charge density  $\sigma$  will remain constant, and in the limit of small  $D$  the number density of monovalent counterions between the two surfaces will approach a uniform value of  $2\sigma/eD$ . Thus, from Eq. (12.44) the limiting pressure in this case is

$$P(D \rightarrow 0) = kT \sum_i \rho_{mi} = -2\sigma kT/zeD \quad (12.53)$$

and

$$W(D \rightarrow 0) = (-2\sigma kT/ze) \log D + \text{constant} \quad (12.54)$$

that is, as  $D \rightarrow 0$  the pressure and the energy become infinite. Note that this is the same limiting pressure as in the case of no bulk electrolyte (counterions only), obtained in Eq. (12.23), and results purely from the limiting osmotic pressure of the ‘trapped’ counterions. Indeed, this is part of an even more general rule for surfaces of constant charge which states that in the (ideal) limit of small  $D$ , all double-layer forces tend towards the osmotic limit,  $P \rightarrow \rho kT$ , where  $\rho$  is the number density of counterions remaining in the gap which is independent of the bulk electrolyte concentration.

If there is counterion binding as  $D$  decreases,  $P$  falls below this limit, and the Poisson–Boltzmann equation must now be solved self-consistently by including the dissociation constants of the adsorbing ions (Section 12.13). The computations have been described by Ninham and Parsegian (1971), and a simple numerical algorithm has been given by Chan *et al.* (1976, 1980b).

The two main effects of a charge-regulating interaction can be summarized qualitatively as follows (see also Healy *et al.*, 1980):

- (i) if counterions adsorb as two surfaces approach each other the strength of the double-layer interaction is always less than that occurring at constant surface charge (Le Chaterlier’s principle), and
- (ii) in general, the interaction potential will lie between two limits, the upper one corresponding to the interaction at constant surface charge and the lower at constant surface potential.

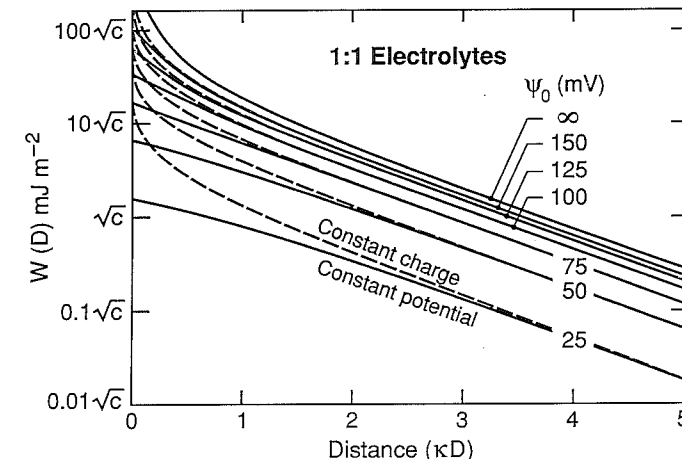


**Fig. 12.10.** Repulsive double-layer interaction energy for two planar surfaces in a 1:1 electrolyte. (Exact solution kindly computed by M. Sculley, R. Pashley and L. White based on Ninham and Parsegian, 1971.)  $\psi_0$  is the potential of the isolated surfaces and  $C$  the electrolyte concentration in  $M$ , which is related to the Debye length by  $1/\kappa = 0.304/\sqrt{C}$  nm. Theoretically, the double-layer interaction must lie between the constant-charge and constant-potential limits. (—, constant charge; —, constant potential). At separations greater than  $1/\kappa$  the forces are well described by Eq. (12.47) for  $z = 1$ .

This is illustrated in Figs 12.10 and 12.11, which show the double-layer interaction potentials of two planar surfaces in 1:1 and 1:2 electrolytes. The curves are based on exact numerical solutions and show the theoretical limits of the constant charge and constant potential interaction in each case. The figure may be used for reading off the interaction energy of any 1:1 or 2:1 electrolyte at any desired concentration  $C$ , and surface separation  $D$ . This is because the energy scales with  $\sqrt{C}$  and the distance scales with the Debye length,  $1/\kappa$ . The constant potential curves of Fig. 12.10 compare reasonably well with the approximate expressions of Eq. (12.47) even at small separations, and especially when  $\psi_0$  is between 50 and 100 mV. However, the accurately computed constant charge interaction is always well above that predicted by the approximate expression at small separations. Approximate expressions for interactions at constant surface charge have been derived by Gregory (1973).

For two surfaces of different charge densities or potentials the interaction energy can have a maximum at some finite distance, usually below  $1/\kappa$ , i.e., the surfaces can *attract* each other at small separations. Approximate equations for the interactions of two surfaces of unequal but constant

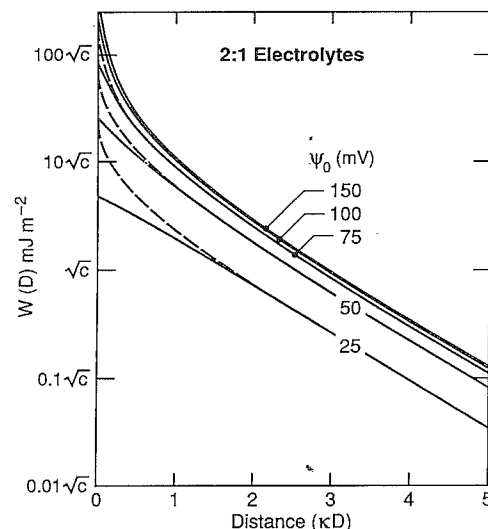


**Fig. 12.11.** Repulsive double-layer interaction energy for two planar surfaces in a 2:1 electrolyte (computed as in Fig. 12.10). The electrolyte concentration  $C$  is related to the Debye length by  $1/\kappa = 0.176/\sqrt{C}$  nm (---, constant charge; ——, constant potential). At separations greater than  $1/\kappa$  the forces are well described by Eq. (12.47) for  $z = 2$ .

potentials were given by Hogg *et al.* (1966) and, in a different form, by Parsegian and Gingell (1972), and for unequal charges by Gregory (1975).

Finally, it is worth again mentioning that at small distances the PB equation often breaks down: the full electrostatic interaction can become more attractive when ion-correlation forces become important (usually at distances below 2–5 nm) or more repulsive when finite ion-size effects become important (usually at even smaller separations).

#### 12.18 VAN DER WAALS AND DOUBLE-LAYER FORCES ACTING TOGETHER: THE DLVO THEORY

The total interaction between any two surfaces must also include the van der Waals attraction. Now, unlike the double-layer interaction, the van der Waals interaction potential is largely insensitive to variations in electrolyte concentration and pH, and so may be considered as fixed in a first approximation. Further, the van der Waals attraction must always exceed the double-layer repulsion at small enough distances since it is a power-law

interaction (i.e.,  $W \propto -1/D^n$ ), whereas the double-layer interaction energy remains finite or rises much more slowly as  $D \rightarrow 0$ . Figure 12.12 shows schematically the various types of interaction potentials that can occur between two surfaces or colloidal particles under the combined action of these two forces. Depending on the electrolyte concentration and surface charge density or potential one of the following may occur:

- (i) For highly charged surfaces in dilute electrolyte (i.e., long Debye length), there is a strong long-range repulsion that peaks at some distance, usually between 1 and 4 nm, at the *energy barrier*. This is illustrated in Fig. 12.12a.
- (ii) In more concentrated electrolyte solutions there is a significant *secondary minimum*, usually beyond 3 nm, before the energy barrier (Fig. 12.12, upper inset). The potential energy minimum at contact is known as the *primary minimum*. For a colloidal system, even though the thermodynamically equilibrium state may be with the particles in contact in the deep primary minimum, the energy barrier may be too high for the particles to overcome during any reasonable time period. When this happens, the particles will either sit in the weaker secondary minimum or remain totally dispersed in the solution. In the latter case the colloid is referred to as being *kinetically stable* (as opposed to *thermodynamically stable*).
- (iii) For surfaces of low charge density or potential, the energy barrier will always be much lower (Fig. 12.12c). This leads to slow aggregation, known as *coagulation* or *flocculation*. Above some concentration of electrolyte, known as the *critical coagulation concentration*, the energy barrier falls below the  $W = 0$  axis (Fig. 12.12d) and the particles then coagulate rapidly. The colloid is now referred to as being *unstable*.
- (iv) As the surface charge or potential approaches zero the interaction curve approaches the pure van der Waals curve, and two surfaces now attract each other strongly at all separations (Fig. 12.12e).

The sequence of phenomena described above can be described quantitatively (see Worked Example below) and it forms the basis of the celebrated *DLVO theory* of colloidal stability, after Derjaguin and Landau (1941), and Verwey and Overbeek (1948). See also Shaw (1970), Hiemenz (1977), and Hunter (1989).

The main factor inducing two surfaces to come into adhesive contact in a primary minimum is the lowering of their surface potential or charge, brought about by increased ion binding and/or increased screening of the double-layer repulsion by increasing the salt concentration. However, if the surface charge remains high on raising the salt concentration, two surfaces

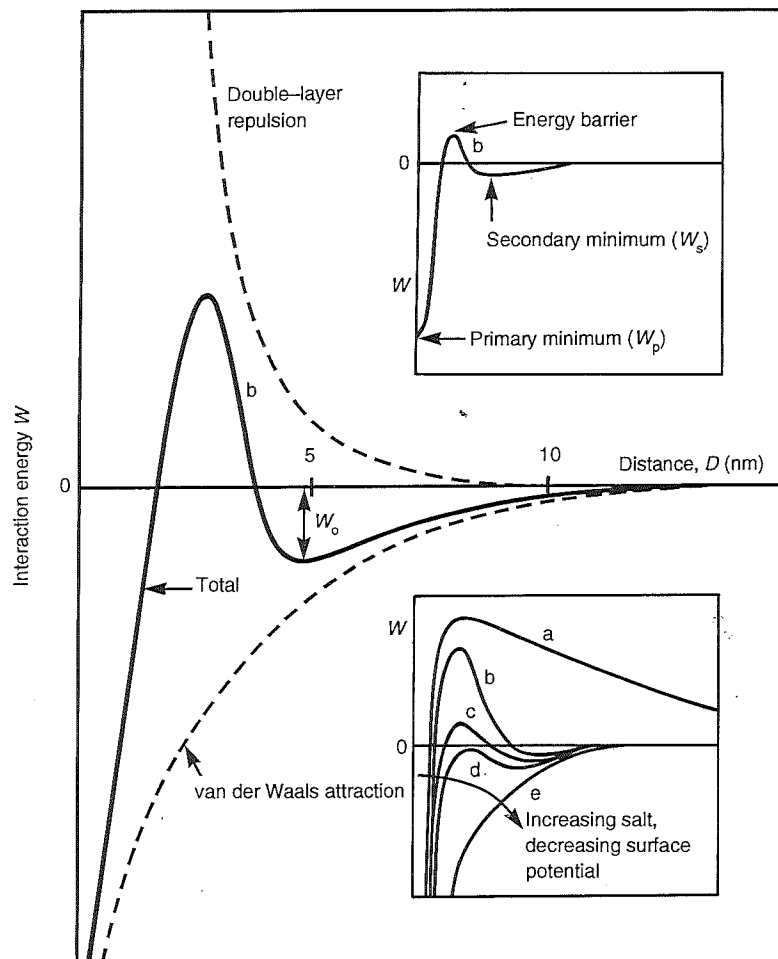


**Fig. 12.12.** Schematic energy versus distance profiles of DLVO interaction. (a) Surfaces repel strongly; small colloidal particles remain 'stable'. (b) Surfaces come into stable equilibrium at secondary minimum if it is deep enough; colloids remain 'kinetically' stable. (c) Surfaces come into secondary minimum; colloids coagulate slowly. (d) The 'critical coagulation concentration'. Surfaces may remain in secondary minimum or adhere; colloids coagulate rapidly. (e) Surfaces and colloids coalesce rapidly.

can still adhere to each other, but in a secondary minimum, where the adhesion is much weaker and easily reversible.

It is clear that one must have a fairly good idea of the charging process occurring at a surface before attempting to understand its double-layer interactions and the stability of colloidal dispersions, as the following example shows.



### ● WORKED EXAMPLE ●

**Question:** For a number of colloidal systems it is found that the critical coagulation concentration varies with the inverse sixth power of the valency  $z$  of the electrolyte counterions, i.e.,  $\rho_\infty(\text{c.c.c.}) \propto 1/z^6$ . Is this empirical observation, known as the *Schultz-Hardy rule*, consistent with the DLVO theory?

**Answer:** The total DLVO interaction potential between two spherical particles interacting at constant potential is

$$W(D) = (64\pi kTR\rho_\infty\gamma^2/\kappa^2)e^{-\kappa D} - AR/6D. \quad (12.55)$$

By definition (see Fig. 12.12d), the critical coagulation concentration occurs when both  $W = 0$ , and  $dW/dD = 0$ . The first condition leads to

$$\kappa^2/\rho_\infty = 384\pi kTD\gamma^2e^{-\kappa D}/A,$$

while the second condition leads to  $\kappa D = 1$ , which shows that the potential maximum occurs at  $D = \kappa^{-1}$  (the Debye length). Inserting this into the above equation leads to

$$\kappa^3/\rho_\infty = 768\pi kT\gamma^2e^{-1}/A,$$

i.e.,

$$\kappa^6/\rho_\infty^2 \propto (T\gamma^2/A)^2.$$

Now, since  $\kappa^2 \propto \rho_\infty z^2/\varepsilon T$ , the above equation implies that

$$z^6\rho_\infty \propto \varepsilon^3 T^5 \gamma^4 / A^2, \quad (12.56)$$

which is a constant if  $\gamma$  is constant, a condition that holds at high surface potentials ( $\psi_0 > 100$  mV) where  $\gamma = 1$  (see Eq. (12.40)). In this limit, therefore,

the critical coagulation concentrations do indeed scale as  $\rho_\infty \propto 1/z^6$ . For example, if coagulation occurs at 1 M with a 1:1 electrolyte, it will occur at  $\frac{1}{64}$  M with a 2:2 electrolyte (or divalent counterions), and at  $\frac{1}{729}$  M with a 3:3 electrolyte (or trivalent counterions). Thus the Schultz-Hardy rule is consistent with the DLVO theory.

But wait. Is it not unreasonable to assume high surface potentials in divalent and trivalent electrolyte solutions? Let us investigate the case of low potentials. Here we have  $\gamma \propto z\psi_0/T$ , so that Eq. (12.56) now becomes

$$z^2\rho_\infty \propto \epsilon^3 T \psi_0^4 / A^2, \quad (12.57)$$

which is constant if  $\psi_0$  remains constant. Thus for low but constant potentials we obtain a modified form of the Schultz-Hardy rule:  $\rho_\infty \propto 1/z^2$ .

In real systems the surface potential is neither high nor constant, but usually falls to quite low values as the valency of the electrolyte counterions increases. For example, if  $\psi_0 \propto 1/z$ , then for low potentials we now obtain:  $\rho_\infty \propto \psi_0^4/z^2 \propto 1/z^6$ , which brings us back to the Schultz-Hardy rule. Clearly the DLVO theory can be applied in more ways than one to explain the Schultz-Hardy rule.  $\square$

### 12.19 EXPERIMENTAL MEASUREMENTS OF DOUBLE-LAYER AND DLVO FORCES

Figure 12.13 shows experimental results of direct force measurements between two mica surfaces in dilute 1:1 and 2:1 electrolyte solutions where the Debye length is large, thereby allowing accurate comparison with theory to be made at distances much smaller than the Debye length. The theoretical DLVO force laws are shown by the continuous curves. The agreement is remarkably good at all separations, even down to 2% of  $\kappa^{-1}$ , and indicates that the DLVO theory is basically sound. One may also conclude that the dielectric constant of water must be the same as the bulk value even at surface separations as small as 2 nm, since otherwise significant deviations from theory would have occurred (Hamnerius *et al.*, 1978, showed that the dielectric constant of water remains unchanged even for 1 nm films). The surface potentials  $\psi_0$  inferred from the magnitude of the double-layer forces agree within 10 mV with those measured independently on isolated mica surfaces by the method of electrophoresis (Lyons *et al.*, 1981). Further, the surface charge density corresponding to these potentials is typically 1e per 60 nm<sup>2</sup>. Thus, at separations below about 8 nm the surfaces are actually closer to each other than the mean distance between the surface charges, and yet the

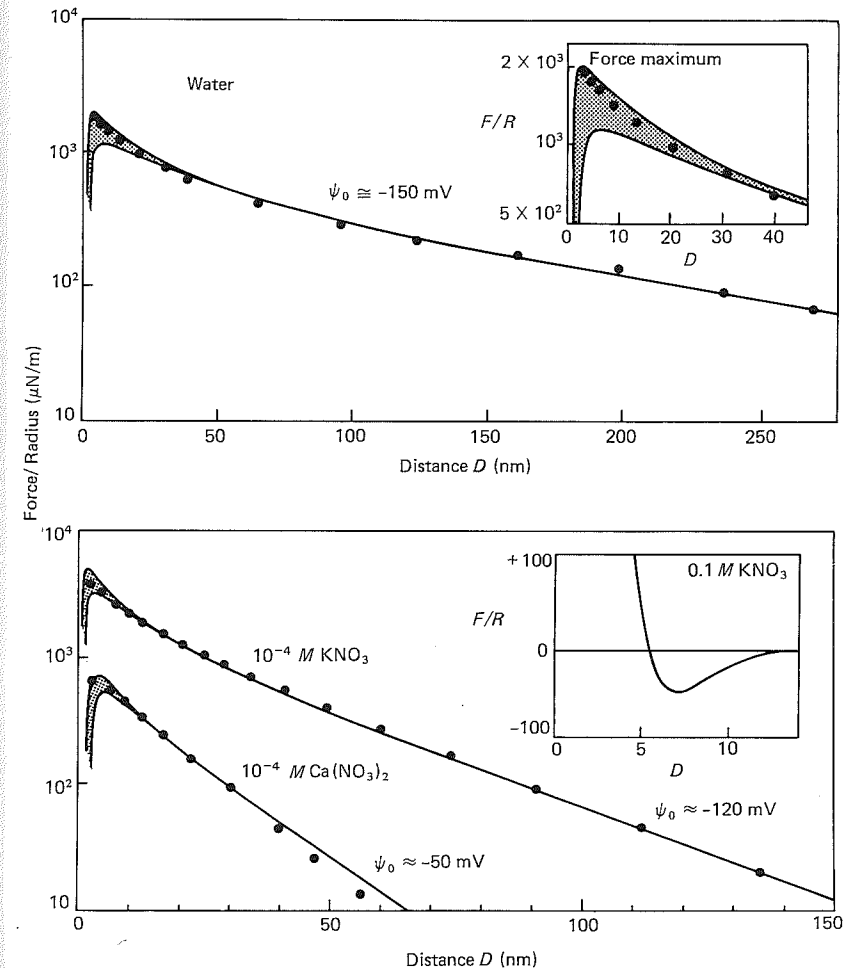
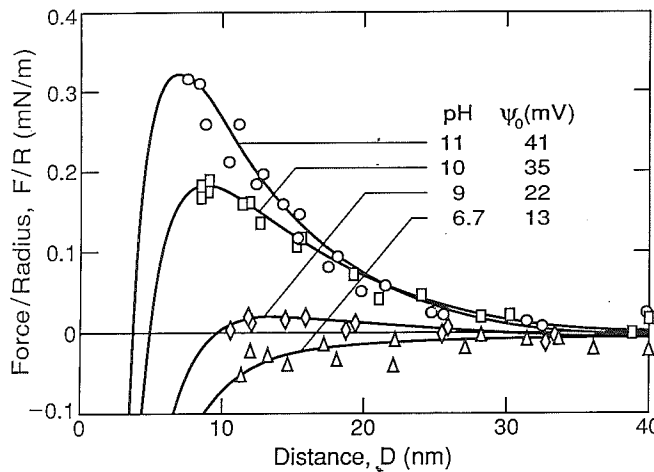


Fig. 12.13. Measured double-layer and van der Waals forces between two curved mica surfaces of radius  $R$  ( $\sim 1$  cm) in water and in dilute  $\sim 10^{-4}$  M  $\text{KNO}_3$  and  $\sim 10^{-4}$  M  $\text{Ca}(\text{NO}_3)_2$  solutions. The continuous curves are the theoretical DLVO forces (using a Hamaker constant of  $A = 2.2 \times 10^{-20}$  J), showing the constant charge and constant potential limits. Theoretically, we expect the interactions to fall between these two limits. (Note that for this geometry the Derjaguin approximation gives  $F/R = 2\pi W$ , where  $W$  is the corresponding interaction energy per unit area between two planar surfaces, as plotted in Figs 12.10 and 12.11.) The inset in the lower part of the figure is the measured force in concentrated 0.1 M  $\text{KNO}_3$  showing the emergence of a secondary minimum. (From Israelachvili and Adams, 1978; Pashley, 1981a; Israelachvili, 1982.)



**Fig. 12.14.** Classic DLVO forces measured between two sapphire surfaces in  $10^{-3}$  M NaCl solutions at different pH. The continuous lines are the theoretical DLVO forces for the potentials shown and a Hamaker constant of  $A = 6.7 \times 10^{-20}$  J (from Horn *et al.*, 1988a).

double-layer forces still behave as if the surface charges were smeared out. The reason for this will become clear in the next section.

Other measurements of double-layer or DLVO forces have been carried out in various 1:1 and 2:1 electrolytes (Pashley, 1981a, b; Pashley and Israelachvili, 1984; Horn *et al.*, 1988a), between surfactant and lipid bilayers (Pashley and Israelachvili, 1981; Marra, 1986b, c; Marra and Israelachvili, 1985), across soap films (Derjaguin and Titijevskaia, 1954; Lyklema and Mysels, 1965; Donners *et al.*, 1977), between silica, sapphire and metal surfaces (Horn *et al.*, 1988a, 1989a, b; Smith *et al.*, 1988), as well as in non-aqueous polar liquids (Christenson and Horn, 1983, 1985). The results are invariably in good agreement with the DLVO theory, often down to separations well below the Debye length.

When deviations do occur these can usually be attributed to the presence of other, non-DLVO, forces or to the existence of a Stern layer (Israelachvili, 1985). A Stern layer of thickness  $\delta$  per surface ( $2\delta$  for both surfaces) can have a profound effect on the DLVO interaction potential because it pushes the plane of origin of the double-layer interaction (the OHP) out to  $D = 2\delta$ . It is remarkable that for values of  $\delta$  as small as 0.2–0.3 nm (corresponding to hydrated sizes of ions) this effect can completely eliminate a deep primary minimum. Instead, the repulsion continues to rise steeply and indefinitely as the surface separation decreases to contact, at  $D = 2\delta$ . This model was first proposed by Frens and Overbeek (1972) to explain the common

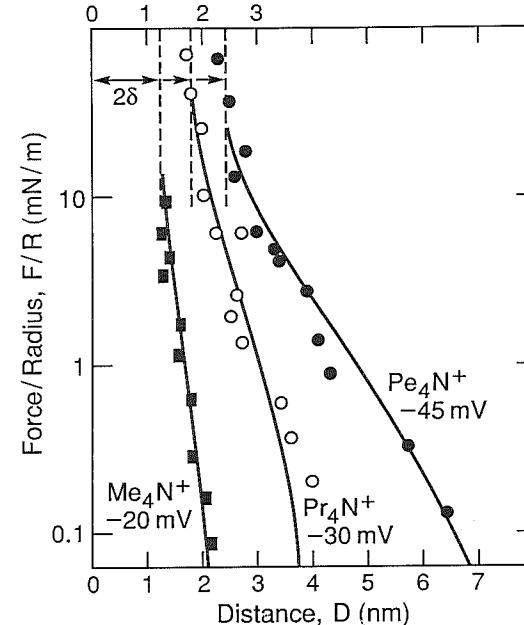


**Fig. 12.15.** Measured forces between two mica surfaces in various tetra-alkyl ammonium bromide solutions (Claesson *et al.*, 1984). The continuous curves are the expected DLVO interactions assuming potentials as shown and Stern-layer thicknesses of  $\delta$  per surface equal to the diameters of the adsorbed cations:  $\delta = 0.6$  nm for methyl ammonium ( $\text{Me}_4\text{N}^+$ ),  $\delta = 0.9$  nm for propyl ammonium ( $\text{Pr}_4\text{N}^+$ ) and  $\delta = 1.2$  nm for pentyl ammonium ( $\text{Pe}_4\text{N}^+$ ). Note how the outward shift in the OHP has eliminated the force maximum and primary minimum, resulting in Stern-layer stabilization.

phenomenon of colloidal stability in high salt, the spontaneous swelling of certain colloids in water, and *repeptization*—the reversible coagulation of colloidal particles (according to the DLVO theory coagulation in a primary minimum should never be reversible). A direct experimental measurement of Stern-layer stabilization is shown in Fig. 12.15 where the counterions used in that study were unusually large.

It is perhaps surprising that measured double-layer forces are so well described by a theory that, unlike van der Waals force theory, contains a number of fairly drastic assumptions, viz. the assumed smearing out of discrete surface charges, that ions can be considered as point charges, the ignoring of image forces, and that the PB equation remains valid even at fairly high concentrations. One reason for this is that many of these effects act in opposite directions and tend to cancel each other out (Section 12.8). As mentioned

above, most experimental deviations in the forces from those expected from the DLVO theory are not due to any breakdown in the DLVO theory, but rather to the existence of a Stern layer or to the presence of other forces such as ion-correlation, solvation, hydrophobic or steric forces. These additional forces, are, of course, very important, especially in more complex colloidal and biological systems where they often dominate the interactions at short range where most of the interesting things happen. Their consideration forms a large part of the rest of this book.

### 12.20 EFFECTS OF DISCRETE SURFACE CHARGES AND DIPOLES

The charge on a solid surface is obviously not uniformly spread out over the surface, as has been implicit in all the equations derived so far. For a surface with a typical potential of 75 mV in a 1 mM NaCl solution, the surface charge density as given by the Grahame equation is  $\sigma = 0.0075 \text{ C m}^{-2}$ , which corresponds to only one charge per  $21 \text{ nm}^2$  or  $2100 \text{ \AA}^2$ . In 0.1 M NaCl the same potential implies  $1e$  per  $2 \text{ nm}^2$ . Thus, the charges on real surfaces are typically 1–5 nm apart from each other on average. What effect does this have on the electrostatic interaction between two surfaces?

Let us consider a planar square lattice of like charges  $q$  as shown in Fig. 12.16a. If  $d$  is the distance between any two neighbouring charges, then the mean surface charge density is  $\sigma = q/d^2$ , and if this charge were smeared out, the electric field emanating from the surface would be uniform and given by  $E_z = \sigma/2\epsilon\epsilon_0$ . What, then, is the field of a surface lattice of discrete charges having the same mean charge density? To compute this field one must sum the contributions from all the charges. The resulting slowly converging series can be turned into a rapidly converging series by using a mathematical technique known as the Poisson summation formula (Lighthill, 1970). If  $x$  and  $y$  are the coordinates in the plane relative to any charge as the origin (Fig. 12.16a), the field  $E_z$  along the  $z$  direction is given by the series (Lennard-Jones and Dent, 1928)

$$E_z = \frac{\sigma}{2\epsilon\epsilon_0} \left[ 1 + 2 \left( \cos \frac{2\pi x}{d} + \cos \frac{2\pi y}{d} \right) e^{-2\pi z/d} + \dots \right], \quad (12.58)$$

where the higher-order terms decay much more rapidly with distance  $z$ . The first term is the same as that of a smeared-out surface charge. The second term is interesting, for it shows that the excess field decays away extremely rapidly, with a decay length of  $d/2\pi$  (e.g., about 0.3 nm for charges 2 nm

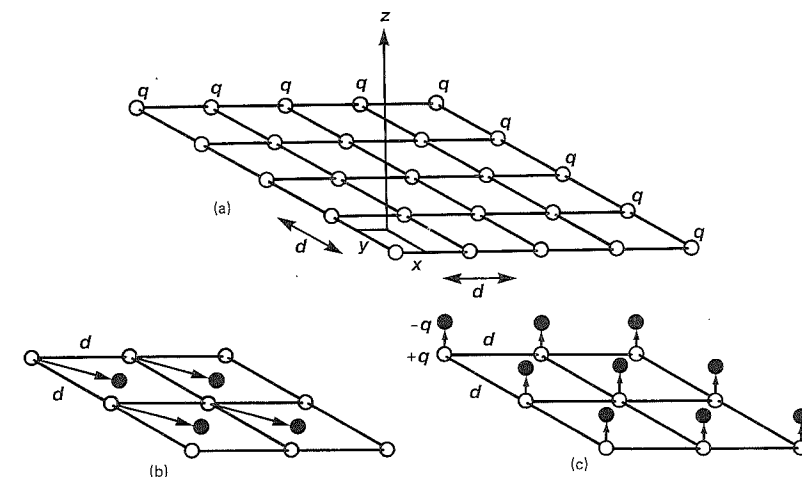


Fig. 12.16. Sections of infinite lattices of charges and dipoles.

apart). Thus, at  $z = \frac{1}{2}d$  the electric field is at most 17% different from that of the smeared-out field, while at  $z = d$  it has reached 99.3% of the smeared-out value! A similar conclusion is reached for other types of lattices; for example, for a hexagonal lattice where neighbouring ions are separated by a distance  $d$ , the mean surface charge density is  $\sigma = 2q/\sqrt{3}d^2$  and the decay length is  $\sqrt{3}d/4\pi$  which is even smaller than for a square lattice implying that the field decays even faster. It is for these reasons that the smeared-out approximation works so well in considering the electrostatic interactions between charged surfaces.

If charges of opposite sign are now added at the centre of each square, as in Fig. 12.16b, the net surface charge density becomes zero. By superimposing the fields of the positive and negative lattices using Eq. (12.58) it is easy to show that the electric field opposite a positive charge (at  $x = 0, y = 0$ ) is

$$E_z = + (4q/\epsilon\epsilon_0 d^2) e^{-2\pi z/d} + \dots, \quad (12.59)$$

while opposite a negative charge (at  $x = \frac{1}{2}d, y = \frac{1}{2}d$ ) it is

$$E_z = - (4q/\epsilon\epsilon_0 d^2) e^{-2\pi z/d} + \dots \quad (12.60)$$

Note that this geometry is equivalent to a dipolar or zwitterionic lattice whose dipoles, of length  $d/\sqrt{2}$  and surface density  $1/d^2$ , are lying parallel to the surface.

For dipoles of length  $l$  comparable to  $d$  arrayed perpendicular to the surface,

as in Fig. 12.16c, the above two equations become replaced by  $E_z \approx \pm (2q/\epsilon\epsilon_0 d^2)e^{-2\pi z/d} + \dots$ . This procedure can be readily extended to other lattices including three-dimensional ionic crystals. The end result is always that the field is positive or negative depending on the  $x$ ,  $y$  coordinates and that it decays very rapidly to zero with increasing  $z$ .

If a second lattice of vertical dipoles is brought up to the first, the Coulombic interaction pressure between the two dipolar surfaces at a separation  $D$  will vary between  $\pm (2q^2/\epsilon\epsilon_0 d^4)e^{-2\pi D/d}$  depending on whether the approaching dipoles are exactly opposite each other or in register (repulsion) or out of register (attraction). The pressure is anyway very small and in reality, since surface dipoles will not be on a perfect lattice but distributed randomly or moving about (e.g., zwitterionic headgroups on a lipid bilayer surface), the net pressure will average to zero in a first approximation, though a Boltzmann-averaged interaction will yield an overall attractive force.

A similar result is obtained if the dipoles are lying in the plane of the surfaces, as in Fig. 12.16b. This is yet another example where the purely electrostatic interaction between a system of charges or dipoles that are overall electrically neutral produces an attractive force, even though intuitively one might have expected two surfaces with vertical dipoles to always repel each other. In the limit where the surface-bound dipoles are free to rotate in all directions the resulting interaction energy must be the same as the attractive van der Waals–Keesom interaction, which decays as  $1/D^4$  (Eq. (11.42)) but is screened if the interaction occurs across electrolyte solution (Section 11.8).

Jönsson and Wennerstrom (1983) pointed out that the total interaction between two dipolar surfaces must also include the image forces of each dipole and its image reflected by the other surface. For two dipolar surfaces of low dielectric constant interacting across water the resulting image force between them can be large and repulsive. They showed that depending on the positional and orientational correlations of the dipoles on each surface the resulting pressure can decay either exponentially or with the inverse fourth power of the separation. Such situations are expected to arise when zwitterionic lipid bilayers and biological membranes ( $\epsilon \approx 2$ ) interact in water ( $\epsilon \approx 80$ ), and these purely electrostatic forces have been proposed to be responsible for some of the repulsive short-range ‘hydration’ forces measured between lipid bilayers in aqueous solutions (cf. Fig. 12.5 and Chapter 18).

#### PROBLEMS AND DISCUSSION TOPICS

**12.1** A glass surface is exposed to water vapour at 96% relative humidity (i.e.  $p/p_{\text{sat}} = 0.96$ ). Estimate the equilibrium thickness  $D$  of the thin film of

water adsorbed on the surface assuming (i) that only electrostatic double-layer forces are operating and that the surface is fully dissociated with a surface charge density of  $\sigma = -0.1 \text{ C m}^{-2}$ , (ii) that the monovalent counterions ( $z = 1$ ) are uniformly distributed throughout the thin water film. With these same assumptions also estimate the repulsive electrostatic pressure between two such planar surfaces immersed in water at a distance  $2D$  apart. Is your estimate likely to be too high or too low, and how does it compare with the attractive van der Waals pressure between the surfaces at this separation? Will the van der Waals attraction eventually win out at some smaller, but physically realistic, plate separation?

**12.2** Calculate the repulsive pressure between two charged surfaces in pure water where the only ions in the gap are the counterions that have come off from the dissociating surface groups (i.e. no electrolyte present, no bulk reservoir). Assume a surface charge density of one electronic charge per  $0.70 \text{ nm}^2$  and  $T = 22^\circ\text{C}$ . Plot your results as pressure against surface separation in the range  $0.5$ – $18 \text{ nm}$  and compare these with the experimental results of Cowley *et al.* (1978) where in Fig. 4b on p. 3166 the authors plot their measured values for such a system ( $\Delta$  points). What conclusions do you arrive at concerning the ‘hydration’ forces between two pure phosphatidylglycerol bilayers at small separations?

**12.3** Show that the double-layer repulsion between two surfaces with low but unequal surface potentials  $\psi_1$  and  $\psi_2$ , viz.  $\gamma_1$  and  $\gamma_2$ , is

$$P = 64kT\rho_\infty\gamma_1\gamma_2 e^{-\kappa D} \quad (12.61)$$

which reduces to Eq. (12.46) when  $\gamma_1 = \gamma_2$ .

**12.4** Consider a colloidal dispersion of large spherical particles suspended in a  $0.1 \text{ M NaCl}$  solution where the Hamaker constant between the particles in the solution is  $A = 10^{-20} \text{ J}$ , and where experimentally it has been established that for the particle-solution interface the surface potential  $\psi_0$  falls linearly with pH from  $\psi_0 = -100 \text{ mV}$  at pH 7, to  $\psi_0 = 0$  at pH 5. Assuming that the spheres are quite large, i.e. that  $R \gg D$  in the range of interest, calculate the range of pH at which the colloid will become ‘unstable’, i.e. where rapid coagulation will occur.

**12.5** The reason(s) why positively charged divalent counterions are better coagulants or flocculants of negatively charged surfaces or particles than monovalent ions is because of one or more of the following:

- (i) They screen the electrostatic repulsion better.
- (ii) They are more hydrated.
- (iii) They bind more easily and hence lower the surface charge more easily.

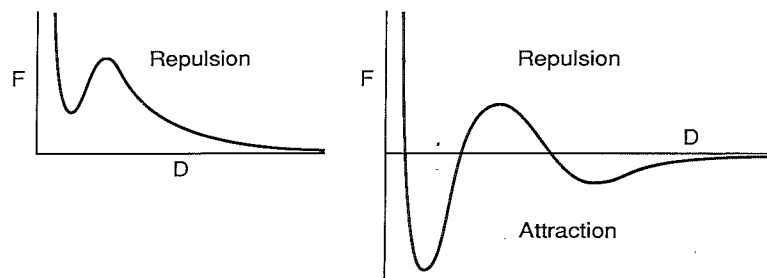


Fig. 12.17.

- (iv) They have additional ion-correlation attractive forces.
- (v) They can bridge two surfaces by virtue of having two charges.
- (vi) They disrupt the water structure more effectively.
- (vii) They have a lower kinetic energy.\*
- (viii) They dehydrate surfaces on binding to them.
- (ix) They enhance the hydrophobic attraction.

**12.6** Two different types of force laws between colloidal particles in an aqueous solution are as shown in Fig. 12.17. Describe how such potentials can arise. If the potentials are assumed to be independent of temperature, sketch how the temperature-composition phase diagrams could look like for these colloidal systems.

**12.7** How does the existence of an electric double-layer contribute to the lateral surface pressure of a fully charged surfactant monolayer at a water surface? Consider two limiting cases: (i) the monolayer is totally insoluble so that all the surfactant molecules remain in the monolayer when it is compressed (in this case the lateral pressure varies with area  $A$ , and is denoted by  $\Pi$ ); and (ii) the monolayer is soluble and so can exchange and equilibrate with the fixed surfactant concentration in the bulk solution (in this case the double-layer contribution to the pressure is independent of area and may be denoted by  $\gamma_{el}$ ).

(Hint: First obtain an expression for the energy of a single double layer, giving careful thought to the reference state. Refer to Payens (1955), Chan and Mitchell (1983), and Hunter (1989, Chapter 7).)

**12.8** When an electric field is applied across an electrolyte solution containing charged particles they are seen to move parallel or antiparallel to the field depending on the sign of their charge. Now, since almost all of the potential drop must occur across the double layer at each electrode surface, there can be no electric field within the conducting electrolyte solution

and hence no force on the charged colloidal particles. Why, then, do the particles move?

**12.9** Split the double-layer interaction free energy into its enthalpic and entropic components and discuss the implications of your result.